Elsevier Editorial System(tm) for Membrane Science
Manuscript Draft

Manuscript Number: JMS-11670R1

Title: THERMALLY TREATED COPOLY(ETHER-IMIDE)S MADE FROM BPDA AND ALIFATIC PLUS AROMATIC DIAMINES. GAS SEPARATION PROPERTIES WITH DIFFERENT AROMATIC DIAMIMES.

Article Type: Full Length Article

Keywords: Copoly(ether-imide) membrane; SAXS; Phase segregation; Thermal treatment; Gas separation

Corresponding Author: Professor Dr. Antonio Hernandez Gimenez,

Corresponding Author's Institution: Dpto. Termodinamica y Fisica Aplicada

First Author: Alberto Tena

Order of Authors: Alberto Tena; Angel Marcos-Fernández; Angel E Lozano; José G de la Campa; Javier de Abajo; Laura Palacio; Pedro Prádanos; Dr. Antonio Hernandez Gimenez

Abstract: A set of copoly(ether-imide)s, formed by the reaction between an aromatic dianhydride (BPDA), a polyoxyalkyleneamine (poly(ethylene oxide) diamino terminated) (PEO-2000) and various aromatic diamines (PPD, BNZ, and ODA) under different thermal treatments, has been obtained and characterized. The existence of phase segregation in these copolymers has been confirmed by SAXS. It has also been proved that aromatic diamines having a hinge group, such as ODA, produce bigger segregated domains while short and rigid aromatic diamines give higher percentages of phase segregation.

A direct relationship between gas permeability and percentage, and size of the domains, of the segregated phase has been obtained. Also, higher or similar selectivities have been observed as a function of the thermal treatment. In such way, the use of high temperatures during the thermal treatment, responsible of the improvement of the phase segregation, enhances the gas properties, producing materials with permeability/selectivity values close to the Robeson limit. In the case of the CH4/N2 pair an interesting reverse selectivity has been observed probably due both to a specific interaction of the gas with the polymer and to an increase in the solubility of CH4 in the soft segregated portions of the copolymer.

The use of PPD as comonomer provides more phase segregation while the use of ODA gives bigger segregated domains. In terms of permselectivity the performances, for all the pairs of gases studied, follow the PPD>BNZ>ODA sequence when relatively low treatment temperatures are used whilst quite similar results for BNZ and ODA were observed when higher treatment temperatures are employed. This seems to indicate that the domains size is a key factor in the gas separation properties with a certain influence of the percentage of segregation. An adequate balance of short length with limited rigidity of the aromatic part should improve the properties of this kind of materials.

Journal of Membrane Science; MEMSCI-S-11-00821

THERMALLY TREATED COPOLY(ETHER-IMIDE)S MADE FROM BPDA AND ALIPHATIC PLUS AROMATIC DIAMINES. DEPENDENCE OF GAS SEPARATION PROPERTIES ON THE AROMATIC DIAMINE.

Highligts

- Copoly(ether-imide)-aromatic/aliphatic membranes have been manufactured.
- Phase segregation) after different thermal treatments has been confirmed by SAXS.
- Thermal treatment and segregation improves the permselective properties.

Graphical Abstract

Graphical Abstract (Figure_GraphAbst_1.tif)

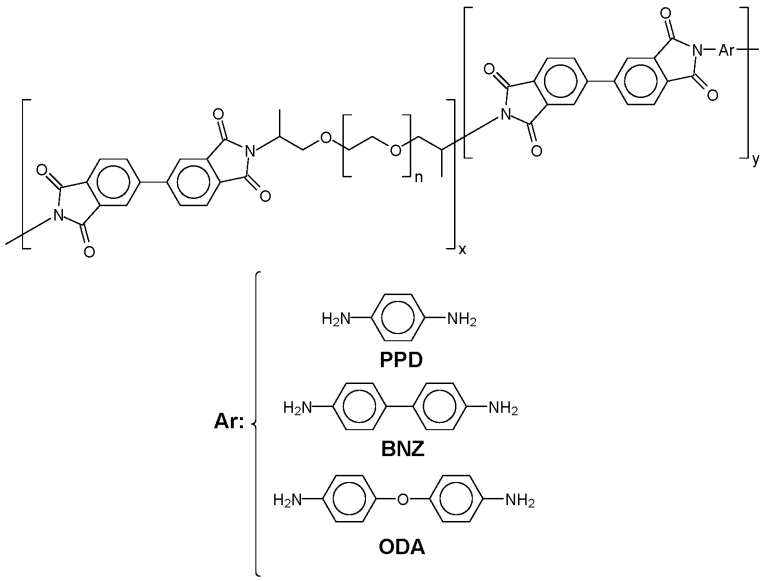

THERMALLY TREATED COPOLY(ETHER-IMIDE)S MADE FROM BPDA AND ALIPHATIC PLUS AROMATIC DIAMINES. DEPENDENCE OF GAS SEPARATION PROPERTIES ON THE AROMATIC DIAMINE.

Alberto Tena[1], Angel Marcos-Fernández[1,2], Angel E. Lozano[1,2], Jose G. de la Campa[1,2], Javier de Abajo[1,2], Laura Palacio[1], Pedro Prádanos[1], Antonio Hernández[1*]

[1]*SMAP UA-UVA_CSIC, Universidad de Valladolid, Facultad de Ciencias, Real de Burgos s/n, 47071 Valladolid, Spain*

[2]*Instituto de Ciencia y Tecnología de Polímeros, CSIC, Juan de la Cierva 3, 28006 Madrid, Spain*

Summary

A set of copoly(ether-imide)s, formed by the reaction between an aromatic dianhydride (BPDA), a polyoxyalkyleneamine (poly(ethylene oxide) diamino terminated) (PEO-2000) and various aromatic diamines (PPD, BNZ, and ODA) under different thermal treatments, has been obtained and characterized. The existence of phase segregation in these copolymers has been confirmed by SAXS. It has also been proved that aromatic diamines having a hinge group, such as ODA, produce bigger segregated domains while short and rigid aromatic diamines give higher percentages of phase segregation.

A direct relationship between gas permeability and percentage, and size of the domains, of the segregated phase has been obtained. Also, higher or similar selectivities have been observed as a function of the thermal treatment. In such way, the use of high temperatures during the thermal treatment, responsible of the improvement of the phase segregation, enhances the gas properties, producing materials with permeability/selectivity values close to the Robeson limit. In the case of the CH_4/N_2 pair an interesting reverse selectivity has been observed probably due both to a specific interaction of the gas with the polymer and to an increase in the solubility of CH_4 in the soft segregated portions of the copolymer.

The use of PPD as comonomer provides more phase segregation while the use of ODA gives bigger segregated domains. In terms of permselectivity the performances, for all the pairs of gases studied, follow the PPD>BNZ>ODA sequence when relatively low treatment temperatures are used whilst quite similar results for BNZ and ODA were observed when higher treatment temperatures are employed. This seems to indicate that the domains size is a key factor in the gas separation properties with a certain influence of the percentage of segregation. An adequate balance of short length with limited rigidity of the aromatic part should improve the properties of this kind of materials.

Keywords: Copoly(ether-imide) membrane; SAXS; Phase segregation; Thermal treatment; Gas separation

*to whom correspondence should be addressed. membrana@termo.uva.es

1. Introduction

Due to environmental concerns and economic interests, there is an imperative need for new materials with improved properties for gas separation applications [1-4]. In particular, the separation of CO_2 from its sources in power plants, steel, cement production plants and the chemical industry, among other industries, has attracted worldwide attention and an enormous amount of research due to that the greenhouse effect, generated mainly by the burning of fossil fuels in the last two centuries, is not being controlled. This greenhouse effect, which is accepted to be the reason of the climate change, is caused by the emission of various gases, most notably carbon dioxide. In the last years, it is mandatory and widely accepted to take account of it in order to stave off or at least to minimize the adverse effects that are expected for the next decades [5-9]. Thus, there is an imperative need of improving the efficiency in old energy sources as coal plants, and in new ones as in the derived from the so-known hydrogen economy, where a fossil fuel (mainly natural gas or coal) is reconverted into hydrogen along with the formation of carbon dioxide. This improvement of efficiency, combined with the position supported by many governments of taxing the emission of greenhouse gases, is forcing both to the academy and the industry to make research in the sequestration of CO_2. Therefore, new technologies must be found in order to separate such gases from diverse mixtures of gases in an efficient way. In this context, the technology of gas separation by membranes is considered a viable option. Gas separation membranes are very competitive attending to economical reasons, with good mechanical properties and excellent gas productivity (flux and ability to separate complex mixtures of gases), they are very easy to install and maintain and because of its efficiency, membranes show small carbon footprint [10,11].

Consequently, all separations where CO_2 is involved have a high social and economical interest because this gas is present as a contaminant or by-product in many industrial processes. Even though many systems have been tested, some of them presenting outstanding properties when compared with other ones developed 20 or 30 years ago, it is crucial, in order to accomplish the challenges need to fit the requirements of the industry, to study more thoroughly the chemical and physical properties of the materials used to make gas separation membranes, and to shed light on the effect of these properties in the separation of gases.

Glassy polymers and in particular polyimides are well known for their excellent thermal oxidative stability and exceptional mechanical properties, along with an extraordinary ability of separating complex mixtures of gases in diverse applications [12-14]. Thus, among all the polymeric membranes, it has been widely demonstrated that the use of aromatic polyimides is one of the best alternatives [15-19]. However, the manufacture of new polymeric materials tailored for more specific applications is needed today. With regards to the separation of CO_2, aromatic polyimides are close to the trade-off of gas permeability versus gas selectivity obtained by Robeson in 1991 [19] but far away from the new one established in 2008 [20]. It should be commented at this point that not many materials have been capable to overpass and even to reach the cited 2008 Robeson limit [22,23] and hence, in order to achieve more serious enhancements in this fields, additional studies should be started.

There are a number of possible itineraries addressed to improve the permeability and selectivity of gas separation membranes. One of them consists of optimizing the structure of the polymer chains in solid sate to give high fractional free volume fractions with a well tailored distribution of sizes and with restrictive or selective channels communicating the voids in order to increase the diffusivity. Other possible approach consists of attempting to increase the solubility introducing a certain chemical affinity for a gas to make it to adsorb on certain moieties of the polymer [17,24]. The introduction of polar groups that can interact favourably with CO_2, such as amine [18] or carboxyl [19] groups has proved to be a very efficient approach to increase the CO_2/N_2 or CO_2/CH_4 selectivity. In this regard, poly(ethylene oxide) (PEO) is a very attractive polymer due to the strong affinity of CO_2 towards the oxygen of the oxyethylenic segments [25-29]. Thus, recently, there have been some studies devoted to the application of polymeric membranes containing PEO or similar polar ether segments in carbon dioxide separations as a result of the enhanced CO_2 solubility of the PEO moieties [30-32].

The use of PEO, which as a very low Tg and a strong ability to crystallize, forces to design materials where physical or chemical crossslinking appears in the polymer material in order to improve the mechanical strength and the membrane stability along the time. Okamoto et al, designed long ago a new generation of block aliphatic aromatic

copolymers with PEO units where the aromatic parts are linked in solid state through charge transfer complex, CTC, interactions (as in whole aromatic polyimides) what produced materials with excellent mechanical properties and admirable ability to separate carbon dioxide from other gases [33-37].

Under these assumptions, this paper studies a series of aromatic-aliphatic copolyimides, in particular poly(ether imide)-segmented co-polymers consisting of micro-domains of rubbery PEO segments and of glassy polyimide segments in such a way that permeation occurs preferentially through rubbery PEO domains [33,34,38].

In previous papers, it has been demonstrated that, for copoly(ether-imide)s with long poly(ethylene oxide) chains of 6000 g/mol, the phase separation morphology of these copolymers can be largely improved by the use of thermal treatments [39-41]. This thermal conditioning leads to an improvement on the gas permeation properties [40]. However, when these long PEO sequences segregate, PEO is able to crystallize which is a serious drawback because permeability decreases. The crystallization process was studied and a dependence of the amount of crystallized PEO with the temperature used in the treatment was determined. In the work presented here, we have used a shorter diamine terminated PEO, 2000 g/mol, as the soft segment, in order to avoid PEO crystallinity. To build the hard segments, PEO-2000 and the rigid aromatic dianhydride has been combined with three different aromatic diamines of different rigidity to study the effect of the aromatic part on the phase separation and the resulting properties. The PEO/aromatic amine ratio was fixed in 2/1 by weigth, resulting in a PEO weight percent from around 35 to 44% in the final copolymer, proportion that has been considered high enough to produce good permeation properties without compromising the superb mechanical properties of the resulting copolyimides.

These aromatic-aliphatic copolymers behave as multi-block polymers that segregate in two phases [38-41]. An exhaustive study of the properties of the synthesized copolyimides (as films obtained by the deposition-evaporation method) containing different aromatic diamines, has been carried out by ATR-FTIR, DSC, TGA, TMA, and SAXS after thermal treatment at different temperatures. The corresponding permeability, solubility, diffusivity and selectivity for different gases have also been studied. This work is part of an intensive study of this kind of materials which will

permit to design materials with improved capability to separate condensable gases and in particular CO_2.

2. Experimental

2.1. Chemicals

p-Phenylenediamine (PPD), 4,4'-diaminobiphenyl (BNZ), 4,4'-oxydianiline (ODA) and 3,3′,4,4′-biphenyltetracarboxylic dianhydride (BPDA) were purchased from Aldrich. These products were purified by sublimation at high vacuum just before being used. Bis(2-aminopropyl) poly(ethylene oxide) 2000 (Jeffamine ED 2003) with nominal molecular weight of 2000 g/mol was kindly donated by Huntsman (Holland). This polyether was dried at 70ºC in vacuum for 5 hours and stored in a desiccator under vacuum until use. Anhydrous N-methylpyrrolidinone (NMP), to be used as polymerization solvent, was purchased from Aldrich. Figure 1 shows the chemical structure of the monomers.

2.2. Synthesis of copoly(ether-imide)s

The polymer samples were synthesized by combination of the dianhydride BPDA with the aliphatic diamine, PEO-2000, and the aromatic diamine (PPD, BNZ and ODA). The procedure for the synthesis of all the polymers in this study was as follows:

a) A mixture of Bis(2-aminopropyl) poly(ethylene oxide) 2000 (*x* mmol), PEO-2000, and the aromatic diamine (PPD, BNZ or ODA) (*y* mmol) in a weight ratio 2:1, was dissolved in anhydrous NMP ((x+y)=5 mmol in 10 mL of NMP) in a three-necked flask blanketed with nitrogen (see Table I).
b) The reaction mixture was cooled down to 0ºC, and under mechanical stirring, a stoichiometric amount of BPDA dianhydride (*5* mmol) was added all at once and the mixture was stirred overnight at room temperature. During this time the dianhydride completely dissolved and the solution reached high viscosity.
c) The resultant viscous copolyamic acid solution was diluted with NMP to the appropriate viscosity for casting, filtered through a nominal number 1 fritted glass funnel, degassed, and cast onto levelled glass plates. The resulting films were covered with a conical funnel to avoid a fast evaporation of the solvent,

dried at 80ºC overnight, and finally treated at 120ºC for 6 hours in a oven under vacuum.

d) Films were obtained of the copolymers with thickness in the range from 60 to 160 μm. Afterwards, thermal treatments under an inert atmosphere of nitrogen were carried out at different temperatures.

The broad distribution of the thickness of the resulting membranes is a consequence of the membrane preparation procedure that needs similar adequate viscosities reached by using different concentrations of the casting solution of each polymer. This variability in thicknesses is not uncommon in literature, and even if we look only at the papers published on copoly(ether-imide)s we can find this broadness frecuently as for example in the early paper of Okamoto et al. [33], where the authors made films of 50-170 microns, to more recent papers [38] where Hangzheng et al made films of 50-150 microns. It should be commented that the thickness of the cast films has not any significant effect on permeation.

The resulting copolymers can be named with the acronym cPI before the starting aromatic diamine: PPD, BNZ and ODA (cPI-PPD, cPI-BNZ, cPI-ODA). Aliphatic PEO content in the final copolymer is 42.9, 43.7 and 34.6% by weight respectively.

2.3. Characterization Methods

Attenuated total internal reflectance-Fourier transform infrared analyses (ATR-FTIR) were performed at room temperature using a PerkinElmer Spectrum One infrared spectrometer equipped with an ATR accessory.

A Thermal Analysis Q500 instrument was used for thermogravimetric analysis (TGA). Disc samples cut from films with weights between 5 and 15 mg were tested. When running dynamic scans, it was done in High Resolution (HiRes) mode, where the heating rate is automatically adjusted in response to changes in the rate of weight loss, which results in improved resolution [42], with an initial heating rate of 10ºC/min under a flux of nitrogen.

Differential scanning calorimetry (DSC) analyses were carried out in a Mettler Toledo (DSC 822e) calorimeter equipped with a liquid nitrogen accessory. Disc samples cut from films weighting 5–15mg were sealed in aluminium pans. Samples were heated with the following cyclic method in order to monitor the changes in thermal properties with thermal treatment: from 25ºC, the sample was heated at 10ºC/min to a target temperature; once reached, the sample was cooled at the maximum cooling rate accessible for the instrument to -90ºC, held at this temperature for 15 min and reheated at 10ºC/min to the next target temperature. The procedure was followed until the last treatment temperature was reached and a final run from -90ºC to 80ºC was performed. In this way, in each heating run, the thermal properties for the copolymers, after treatment to the previously reached temperature, were obtained.

Thermomechanical (TMA) tests were performed in a Rheometric Scientific instrument model DMTA V. Rectangular test pieces of 3 mm width and 20 mm length were cut from films. A distance of 10 mm was set between fixation clamps. Runs were carried out from ambient temperature at 2ºC/min with a static stress of 3 MPa.

SAXS measurements were performed at the beamline BM16 at the European Synchrotron Radiation Facility (Grenoble, France). Wave length of the X-ray beam was 0.980 Å. Detector calibration was done with silver behenate ($AgC_{22}H_{43}O_2$). Disc samples cut from films were placed in a Linkam ® hot stage and heated at 10ºC/min while the SAXS spectra were recorded. Calibration of temperature gave a difference of approximately 7ºC between the temperature reading at the hot stage display and the real temperature at the sample.

Tensile properties were measured in a MTS Synergie 200 testing machine equipped with a 100 N load cell. Rectangular test pieces of 3.5 mm width and 25 mm length were cut from films. A crosshead speed of 5 mm/min was used. Strain was measured from crosshead separation and referred to 10 mm initial length. At least six samples were tested for each copolymer at room temperature.

2.4. Gas Permeation and Selectivity

The permeability, P, for O_2, N_2, CO_2 and CH_4 were determined by using a permeation device with constant volume and variable pressure which uses the *time-lag* operation method. The measurements were carried out at 3 bar and 30 ºC. A sketch of the device used has been shown elsewhere [43].

The strategy known as ‘‘time-lag’’ method is attributed to Daynes et al. [44] and it is especially appropriate to determine permeability and diffusivity of a sample by a simple, rapid and accurate method working under transitory regime. The method has been successfully applied to polymer permeation by many authors [45,46]. Its theoretical framework, as well as the practical possibilities and limits of the time-lag technique have been abundantly documented, [47]. It is nowadays an accepted method to assess the permeability and diffusion coefficients of a gas through a polymer film. To sum up, the classical treatment postulates, among other hypothesis, the Fick’s law to hold with a constant diffusion coefficient for a constant thickness membrane thus assuming no swelling of the membrane by the permeant. When these conditions hold, the transitory response at the downstream part of a membrane to a pressure step at the upstream part enables the time-lag, t_0, to be easily computed. This parameter is linked to the diffusion coefficient, D, of the permeant through the simple expression [46]:

$$t_0 = \frac{\Delta x^2}{6D} \qquad (1)$$

Δx being the thickness of the membrane.

The amount of gas transmitted at time t through the membrane is calculated from the permeate pressure, p_2, readings in the low-pressure side. The inherent leak rate in the downstream side determined after evacuating the system has been measured for each experimental run. The permeability coefficient can be obtained directly from the flow rate into the downstream volume upon reaching the steady state. Finally, solubility, S, can be obtained from directly measured permeabilities and diffusivities as follows

$$S = \frac{P}{D} \qquad (2)$$

3. Results and Discussion

3.1. Copoly(ether-imide)s imidization

Poly(ethylene oxide) chains are prone to oxidation [48], and therefore, a great care was taken to carry out the imidization process. After casting the polymer solution, films were dried overnight, and subsequently they were additionally dried on heating at 120ºC for 6 h. It is very important to note that after the 6 h heating at 120ºC the solvent was almost completely removed as proved by thermogravimetric analysis. Moreover, all the copolymers resulted to be insoluble in DMF (N,N-dimethylformamide), DMAc (N,N-dimethylacetamide), NMP (N-methyl-2-pyrrolidinone), hexane, toluene, THF (tetrahydrofuran), CH_2Cl_2 (dichloromethane) after this drying process.

Infrared spectra were recorded to check for the progress of imidization as shown for example in Figure 2 for the copolymer from ODA (cPI-ODA). In this figure, the IR bands centred around 3257, 2500, 1657, 1603 and 1538 cm^{-1} strongly decrease or disappear, and the bands at 1774, 1713, 1372 and 738 cm^{-1} increase or appear after imidization. It can be seen that imidization has been practically completed for these copolymers after treatment at 120 ºC. An additional treatment at 160ºC for short time produced the whole imidization of the polyamic acid to polyimide as it could be clearly observed in the FTIR spectra. No differences appear in the FTIR spectra of samples cured at 160°C and temperatures up to 265 ºC.

This full imidization at relatively low temperatures is quite remarkable and has already been found for copoly(ether-imide)s based on 6000 g/mol PEO segments [40]. For fully aromatic polyimides, very high temperatures, generally above 300ºC are necessary for complete imidization. Two works, studying similar copoly(ether-imide)s to the ones presented here, state that a thermal treatment at 170ºC completely imidize the precursor poly(amic acid)s to polyimides[33,37]. However authors did not show any FTIR characterization to demonstrate the declared whole conversion. In other more recent research, authors affirm, by using AFT-FTIR, that all synthesized poly(amic acid)s are converted to PEO polyimides after a thermal treatment at 200 ^{o}C [38].

3.2. Thermal Stability

Thermogravimetric analysis was performed to evaluate the thermal stability of the synthesized copolymers. Dynamic runs in Hi-Res mode, in a nitrogen atmosphere, showed a weight loss pattern in several steps for all the samples after being treated at 160 ºC for 2 hours (Figure 3).

The behaviour was similar for the different samples. The initial small loss (below a 2% in weight, from ambient temperature to approximately 300ºC) can be attributed to the absorbed water and residual solvent in the sample. This initial loss was higher for the samples treated at 120ºC, where a significant amount of solvent is still retained. Other authors have found the same results in similar copoly(ether-imide)s. In these works it was shown, by TGA-FTIR, that residual solvent plus absorbed water were released after curing at 200ºC and vacuum [49], and 300ºC were necessary to completely eliminate the residual solvent [50]. The second step is thought to be due to the degradation of bis(2-aminopropyl) poly(ethylene oxide) 2000, PEO-2000, included in the copolymer composition, and it is therefore assigned to the loss of the polyether block sequences. The differences between the weight losses should be due to the different mass percentages of PEO in the copolymers. In effect, there was a good agreement between the experimental weight loss (35, 41 and 44% losses for PPD, BNZ and ODA respectively) and what should be expected according to the mass balances (34.6, 42.9 and 43.7% for PPD, BNZ and ODA, respectively). In similar copolymers with the same poly(ethylene oxide) diamino terminated [41], and with longer PEO chains [40], the selective degradation of the polyether chains has been clearly demonstrated. The final stage of weight loss is due to the thermal decomposition of the remaining aromatic polyimide segments, leaving a relatively high amount of carbonaceous residue.

3.3. Calorimetric Studies

The samples treated at 120ºC for 6 hours were heated in a DSC instrument with a cyclic method in order to monitor the changes in thermal properties after a thermal treatment [40]. The changes in the T_g and T_m for PEO chains are shown in Figures 4 and 5 (respectively) as a function of the treatment temperature (the temperature instantaneously reached by the DSC) for the three copolymers studied. No transition related to aromatic polyimide hard segments was detected by DSC.

From figure 4 was clear that T_g changed when the sample was heated up to approximately 200ºC and it remained constant after higher T treatments. These changes were ascribed to an improvement in the phase separation of the copolymers when simultaneously all the remaining solvent was released as found by TGA, which led to purer PEO domains with lower T_g. The final T_g was similar for copolymers BNZ and PPD, with values in the range of pure amorphous PEO, whereas for copolymer ODA, the final T_g value was clearly higher. The T_g of amorphous PEO is reportedly in the range -55 to -70 ºC depending on molecular weight [51]. The higher rigidity of BNZ and PPD diamines seems to produce, in principle, a better phase separated system and therefore a purer PEO phase than the more flexible ODA diamine.

When samples were treated above 200ºC, some PEO crystallinity appeared (see figure 5). This means that PEO domains were very pure, because only pure PEO was able to crystallize. Melting temperature for PEO crystals is similar and very low for BNZ (cPI-BNZ) and PPD (cPI-PPD) copolymers (approximately -5ºC) whereas for ODA copolymer (cPI-ODA) it is much higher (approximately 16ºC) although still far from the melting point of high molecular weight PEO homopolymer [52]. It seems surprising that ODA copolymer, with less pure PEO domains according to the T_g data, had a higher T_m for PEO crystals than BNZ and PPD. However, melting point was strongly influenced by the size of the crystals, thus, higher melting point for ODA copolymer seemed to mean that the size of the PEO domains was bigger than those for BNZ and PPD copolymers, as it will be confirmed later by SAXS measurements.

If a value of 8.67 kJ/mol is taken for the melting enthalpy of PEO [52], the amount of crystallized PEO, in the samples studied in this paper, appeared as almost negligible, less than 1.5% of the PEO contained in the copolymers. When we compare the ODA copolymer with the copolymer of the same structure and virtually the same PEO content in the copolymer, but having longer PEO chains (BPDA 2/1 in reference 40), crystallinity has been reduced after he thermal treatment at 300ºC from 32% to 0.9% by lowering the length of the PEO sequences. In addition, it is worth noting out that at the temperature of measurement of permeabilities and selectivities, the PEO will be melted and hence it will be in a completely amorphous state.

3.4. Thermomechanical Analysis

Thermomechanical analysis was also carried out in order to detect the glass transition temperature of the aromatic polyimide hard segments, which were not detected by DSC. The criterion to determine the T_g of the polyimide segments was the temperature when strain was 10 times that of the sample at 100ºC [40].

The corresponding results for T_g and some temperatures of treatment are shown in Table II. As seen for the PEO segments by DSC, the treatment at higher temperatures raised the T_g of the polyimide segments, what means that phase separation also improved within the hard domains when the remaining solvent in the copolymer is released. It was also evident that the use of the more flexible aromatic diamine, ODA, gave the copolymer with the lowest T_g of this series, and that the bigger length of BNZ seemed to increase the T_g over that of PPD for the rigid aromatic amines. For all the copolymers, the T_g of the aromatic polyimide was well above ambient temperature, although lower than the corresponding T_g for the pure aromatic homopolymer, due to the lower number of structural units (polymerization degree) and, consequently, lower length of the aromatic polyimide segments in the copolymer when compared with the corresponding homopolymer, and also due to the possible inclusion of some PEO segments in the polyimide domains [40].

3.5. Small Angle X-ray Scattering

A single broad peak was obtained in the scattering curves ($I(q)q^2$ vs. q). Two parameters can be calculated from the scattering curves: the relative invariant, Q', as the integral below the curve Iq^2 vs. q, which is related to the extent of the phase separation; and the maximum on the scattering curve, q_{max}.

Q' can be correlated with the electron density of the phases (assuming there are two of them) as:

$$Q' = k\left(\Delta\rho\right)^2 \phi(1-\phi) \qquad (3)$$

where ϕ is the fraction of one of the phases, $\Delta\rho$ is the difference in the electron densities of both phases and K is a constant related to the experimental geometry and the Thomson scattering factor. Changes in Q' may arise from changes in the extent of phase segregation or from changes in the density difference between the phases.

q_{max} is related to the separation of domains or heterogeneities in the material or length scale L. In the simplest analysis for lamellar phases, the scattering may be treated according to Bragg's Law and hence:

$$L = \frac{2\pi}{q_{max}} \tag{4}$$

For not truly lamellar morphologies a calculation from the curve I vs. q should be preferred [53]. In our case we were not interested in the absolute value for this length scale of the segregated phase but rather on the change of this scale with temperature. Thus, this procedure will be followed attending to its higher accuracy on determining the maximum of the scattering curve.

The obtained results for Q' and L, are represented in Figure 6 for the copoly(ether-imide) containing ODA. In the curves shown in Figures 6-a and 6-b for the sample treated at 120ºC, there is a change (steep increase in both the relative invariant and the characteristic length in the segregated phases) that appears in a range from 180 to 220 ° C, which approximately coincides with the decrease in T_g of the PEO phase as seen in Figure 4, and is related to the release of most of the remaining solvent trapped in the copolymers.

The evolution of both parameters stood until the end of the test temperature range, 300 º C. During cooling, this change in slope did not appear, demonstrating that the phase separation was irreversible. The difference between heating and cooling curves for each temperature should correspond to the net change occurred. For the sample heated at 160ºC for 2 hours, the change in Q' (not shown) was very small, meaning that this treatment was enough to almost fully develop the phase separated structure in this

copolymer. The change in L for this sample, Figure 6-b, took place above 220ºC, after T_g of the rigid polyimide segments was surpassed, and it was much lower than the change exhibited by the sample treated at 120ºC. This slower change above 220ºC took place after practically all the residual solvent had been released.

The same behavior was found for copolymers having BNZ and PPD treated at 120ºC, as seen for example in Figures 7-a and 7-b. Q' and L increased from approximately 180ºC until the highest temperature of the test was reached. In the same graphs (crosses), experimental data for samples treated in an oven at 120ºC (6h), 160ºC (2h), 180ºC (2h), 200ºC (2h), 220ºC (2h), 250ºC (1h) and 265ºC (1h) and measured at ambient temperature are included. For these samples, the same trends in Q' and L were found for the samples heated in-situ at the Linkam hot stage.

Figures 8-a and 8-b show the evolution of Q' and L with temperature for all the copolymers. The samples were obtained in situ (SAXS cell) from polymer films previously heated to 120 ºC during 6 h. Note that, to eliminate the influence of the different film thicknesses and electronic density, the relative $Q'_r = Q'(T)/ Q'(\text{baseline at } T)$, is shown in Figure 8-a. Moreover, the influence of the different background and of the differences in the corresponding base lines was also removed by this procedure.

It is seen that PPD containing copolymers gave higher proportion of separated phase while those containing ODA gave bigger phase separated domains. The sequence of the copolymers with increasing Q'_r coincided with the decrease in length of the aromatic diamine.

For the copolymers from BNZ and PPD, the spacing was very similar, and much lower than for copolymer from ODA as shown in Figure 8-b. For these samples treated at 120ºC, when heated up to more than 300 ºC, L increased about a 25% when the diamines are BNZ and PPD, whereas it increased about a 50% for the copolymer having ODA. In summary, the size of the domains decreased with the rigidity of the aromatic diamine used.

A comparison of Figure 5 with the evolution of L as shown in Figure 8-b shows that the melting point increases with the size of the domains, L. This is in accordance with the

predictions of the Gibbs-Thomson law which states that the melting-point of a substance decreases when the curvature radius of cavities decreases (with a proportionality constant depending only on the confined substance in question).

The spacing for copolymer from ODA after the thermal treatment until 300ºC, was about 10 nm when measured at ambient temperature. This value was much lower than the spacing for the same copolymer built from a PEO having Mw= 6000 (L = 18.9 nm) [35], showing that there is a dependence of L with molecular weight of the PEO for this type of copolymers; the longer the polyether the larger the spacing.

3.6. *Mechanical Properties*

SAXS, DSC and thermomechanical studies have shown the changes produced in the morphology of the copolymers during thermal treatment and the changes in their thermal properties. To complete the study on the physical properties of these copoly(ether imide)s, mechanical properties were measured in tensile mode for the copolymers treated at 160ºC for 2 hours. The so obtained results are shown in Table III.

For copolymers from ODA and PPD, yielding of the samples took place at approximately 10% strain. At this point, strain increases with tensile strength almost unchanged until rupture. For copolymer from BNZ, rupture occurred very early, probably because it is the thinnest film (60 µm) and the occurrence of defects is more critical, triggering the rupture. The value of the modulus for ODA containing copolymers was smaller than for the other ones, as expected, because from thermal data it was confirmed a higher degree of mixing between the segments, and therefore, the polyimide hard domains, responsible for the mechanical resistance at the early stages of the test, were softer for ODA copolymer. If we compare the values for ultimate properties for ODA and PPD copolymers, it is seen that the shorter the diamine (PPD), the higher the tensile strength and the lower the ultimate strain. It is worth noting that in all cases the mechanical properties of the material were reasonably good.

3.7. Gas Permeation and Selectivity

Gas permeation measurements showed an improvement in the permeation properties, depending on the thermal treatment used, so that there is a direct relationship between: treatment temperature, phase segregation and permeation properties. An example, showing the increase in permeability of CO_2 with the treatment temperature, is presented in Figure 9 for the BNZ containing copolymer. The permeability versus treatment temperature trend was quite similar for all the copolymers and tested gases. In all cases the increase in permeability was gradual for treatment temperatures up to approximately 160 ºC, according to the increasing release of the remaining solvent and to the improvement in the phase segregation.

For all the copolymers, the selectivity versus diffusivity and the solubility-selectivity term versus the diffusivity-selectivity term for the different pairs of gases and the temperature treatments are shown in Figures 10 to 13. Also the PEO gas separation properties, both for semicrystalline and amorphous PEO, [27] are shown for each gas in these Figures. Note that semicrystalline and amorphous PEO showed the same selectivity and the same kind of selectivity with the same balance of solubility and diffusivity contributions, with a little more relevant contribution of the solubility-selectivity term for both forms of PEO. This seems to indicate that gas separation is fundamentally determined by the properties of the amorphous phase of PEO. Then, the crystalline part of semicrystalline PEO should act as mere inert obstacles to the flux that only reduce permeability [27]. In all cases, the observed tendency was to reach the PEO balance of selectivity (both the solubility and diffusivity terms), as the temperature of treatment increases; i.e. when the phase segregation proceeds. The thermal treatment also approaches the gas permeability value of these copolymers to that of the amorphous PEO.

The Robeson plots are shown in Figures 10-a to 13-a, for O_2/N_2, CO_2/CH_4, CO_2/N_2 and CH_4/N_2. Depicted arrows refer to the direction of increasing treatment temperatures. The Robeson's upper bounds are shown in these plots including both the old limit [20] and the new one [21] when both exist. Nevertheless, note that no Robeson limit has been determined for the CH_4/N_2 gas pair because this selectivity is the opposite of that determined by Robeson. This means that usually N_2 is more permeable than CH_4 while our copolymers showed the opposed trend.

For the CH_4/N_2 Robeson plot, some data taken from the literature [54-59] have been shown in the graphic and a pseudo bond has been drawn based on these data only to give an idea on the best selectivity versus permeability trade-off achieved so far.

The permeability of the gases as a function of the aromatic diamine always followed the order: PPD, BNZ and ODA. Copolyimides from BNZ and ODA gave similar permeabilities when the treatment temperatures were high. When only one of the gases was a condensable one (CO_2/N_2 and CH_4/N_2 gas pairs), the selectivity increased with the temperature of treatment while for the rest of gas pairs (O_2/N_2 and CO_2/CH_4), selectivity decreased slightly with the temperature of treatment. In all cases the tendency went towards the selectivity versus permeability characteristics of amorphous PEO. An exception was observed for the CH_4/N_2 pair where an increase in the phase separation of PEO gives selectivity values over the characteristic gas selectivities of both semicrystalline and amorphous PEO.

When permeabilities and selectivities for the copolymer from ODA were compared with the same copolymer having longer PEO chains (6000 g/mole, PI-43 in reference 39) after a thermal treatment at 250ºC (when phase segregation has been well developed) (see Table IV), it was found that permeability values decreased between 30 and 45%, whereas selectivity values increased between 10 and 19%. These differences can be related to the better phase separation achieved for the copolymer with longer PEO lengths, where, in addition, also the aromatic polyimide segments were longer. Thus, the PEO domains seem to be the main responsible for the permeability, and therefore a less perfect phase separation in the ODA copolymer leads to a reduction in permeability. On the other hand, it could be presumed that polyimide segments influenced the selectivity, and because a higher mixing of polyimide segments in the PEO domains was expected for the copolymer from ODA, a small increase in selectivity was to be expected.

Additional information for the behaviour of these copolymers as gas membranes could be obtained from the analysis of the diffusivity and solubility parameters. It is well established that the diffusivity should decrease with the kinetic diameter of the gas while the solubility can be directly correlated with its critical temperature, [60,61].

These data are shown in Table V, [62,63]. The so-obtained diffusivities and solubilities followed these general trends with the exception of CO_2 that showed a much lower diffusivity than that expected according to its kinetic diameter.

The solubility-selectivity term has been confronted versus the diffusivity-selectivity one for all the membranes and gas pairs studied in Figures 10-b to 13-b. These selectivities terms are defined according to:

$$\alpha_{ij} = \frac{P_i}{P_j} = \frac{D_i S_i}{D_j S_j} = (\alpha_D)_{ij} (\alpha_S)_{ij} \qquad (5)$$

These Figures show that the ideal selectivity, α_{ij}, is mostly determined by the solubility term, $(\alpha_D)_{ij}$, for almost all the copolymers and gas pairs.

It is interesting to observe how the effect of the diffusivity term increased in the ideal selectivity except for the O_2/N_2 pair in the ODA copolymer, which showed a lessening of this term and an increment of the solubility term (as opposed to the other copolymers from PPD and BNZ), when it was increased the treatment temperature. In all cases the solubility and diffusivity contributions to the ideal selectivity approached those of the amorphous PEO. However, the solubility-selectivity factor had a higher effect on the ideal selectivity when there was at least a condensable gas in the studied gas pair. It is curious to note that a tendency to reach the solubility and diffusivity terms of PEO was shown also for the CH_4/N_2 pair, which presents, in the Robeson's plot, higher selectivity values than PEO when higher temperature treatments are employed.

The reverse selectivity of the CH_4/N_2, seen in Figure 13-a, was probably caused by an especially high enhancement of the CH_4 permeability when high temperature treatments were used. This fact could be due to a specific affinity of CH_4 for the segregated domains or their interfaces. In effect, the solubility parameter followed the same sequence than the degree of segregation (PPD ≥ BNZ > ODA), Figure 14-a, while diffusivity followed the tendency observed for the size of the domains, L, Figure 14-b.

4. Conclusions

A new series of copoly(ether-imide)s presenting good gas separation properties have been prepared. These copolymers have been synthesized by the reaction between an aromatic dianhydride (BPDA), a diamine terminated poly(ethylene oxide) having a molecular weight of 2000 g/mole (PEO-2000) and various aromatic diamines (PPD, BNZ and ODA).

FTIR showed that almost complete imidization was achieved at temperatures as low as 120ºC, and that this process was wholly achieved after treatment at 160ºC, which is well below the temperature needed to imidize fully aromatic polyimides. Based on TGA data, these copolymers are stable in inert atmosphere up to 300ºC, with a selective degradation of the polyether segments at higher temperatures. DSC, TMA and SAXS experiments proved the existence of a phase separated morphology in these copolymers, with an amorphous PEO phase at ambient temperature and an aromatic polyimide phase with a T_g well above room temperature. The degree of segregation of the phases followed the trend PPD ≥ BNZ > ODA, whereas the size scale of the morphology followed the reverse ODA > BZN ≈ PPD tendency, showing that less rigid aromatic diamines gave bigger segregated domains while more rigid aromatic diamines gave better phase segregation.

Thermal treatment of the copolymers affects the morphology and, in consequence, the physical properties. Initially, at intermediate treatment temperatures, the release of practically all the remaining solvent in the imidized copolymers produces a fast improvement in the phase separation, while treatments at higher temperatures (up to the degradation temperature) produce a further improvement. The possible variations of monomers, monomer percentages and treatment temperature open a wide range of potential for the optimization of these copoly(ether imide)s and other analogous to tailor materials with excellent functionality in different gas separation applications.

After complete imidization, all the samples show increasing selectivity for the studied pairs of gases. This improvement is due to the high percentage and size of the domains of the segregated phases that determine the extra permeability and selectivity shown at higher treatment temperatures. For the case of CH_4/N_2 an interesting reverse selectivity

appears probably due to a higher selectivity of CH_4 in the soft segregated portions of the copolymer.

The use of PEO-2000 in these aromatic-aliphatic copolyimides produced a significant reduction in permeability and a slight increase in selectivity for all gases studied when they are compared with the analogous copolymers having 6000 g/mol molecular weight PEO, due to a less perfect phase segregation.

In terms of permselectivity, the gas performances, followed the aromatic diamine; PPD>BNZ>ODA sequence when relatively low temperatures of treatment are employed whereas quite similar results for the copolymers from BNZ and ODA were obtained when high temperature treatments were used. This indicated that the segregated domains size seems to be the key factor along with a certain influence of the percentage of segregation. An adequate balance of short length with limited rigidity of the diamine responsible of the aromatic part should improve the gas separation results.

Finally, on comparing the permeability, solubility and diffusivity data with the data referred in the literature for pure PEO, it was concluded that the tendency of these parameters after the improvement of segregation is to approach the data exhibited by pure amorphous PEO (an exception was seen for the CH_4/N_2 gas pair that showed a much larger improvement).

5. Aknowledgements

We are indebted to the Spanish Junta de Castilla León for financing this work through the GR-18 Excellence Group Action and to the Ministry of Science and Innovation in Spain for their economic support of this work (MAT2008-00619/MAT, CIT-420000-2009-32 and MAT2010-20668/MAT). We also acknowledge financial support from the programme Consolider Ingenio 2010 (project CSD-0050-MULTICAT).

Authors thank the access to the beamline BM16 at the European Synchrotron Radiation Facility (ESRF) in Grenoble (France). We are grateful to Dr. Ana Labrador and Dr. François Fauth for their help at BM16 station at the ESRF. The help provided by Sara

Rodriguez in measuring gas permeability and selectivity is greatly appreciated. A. Tena thanks CSIC for a predoctoral JAE fellowship.

6. References

1. W.J. Koros, Gas separation membranes: Need for combined materials science and processing approaches, Macromol. Symp. 188, 13–22 (2002)

2. P. Pandey, R.S. Chauhan, Membranes for gas separation, Prog. Polym. Sci., 26 (2001) 853-893

3. M. Ulbricht, Advanced functional polymer membranes, Polymer 47 (2006) 2217–2262

4. L.M. Robeson, Polymer membranes for gas separation, Curr. Opin. Solid State Mater. Sci. 4 (1999) 549–552

5. R. Steeneveldt, B. Berger, T.A. Torp, CO_2 capture and storage. Closing the knowing–doing gap, Chem. Eng. Res. Des. 84 (2006) 739–763

6. A. Meisen, X. Shuai, Research and development issues in CO_2 capture, Energy Convers. Manage., 38, (1997) 37-42

7. D. C. Victor, Strategies for cutting carbon, Nature 395 (1998) 8837-38.

8. J. D. Figueroa, T. Fout, S. Plasynnski, H. McIlvried, R.D. Srivastava, Advances in CO_2 capture technology—The U.S. Department of Energy's Carbon Sequestration Program, Int. J. Greenhouse Gas Control, 2 (2008) 9-20

9. H. J. Herzog, What future for carbon capture and sequestration? Environ. Sci. Technol. 35 (2001) 148-153

10. H. Lin, B.D. Freeman, Materials selection guidelines for membranes that remove CO2 from gas mixtures, J. Mol. Struct. 739 (2005) 57–74

11. R.W. Baker, Future directions of membrane gas separation technology, Ind. Eng. Chem. Res. 41 (2002) 1393–1411

12. M.T. Bessonov, M.M. Koton, V.V. Kudryavtsev, L.A. Laius, Polyimides: Thermally Stable Polymers, Consultants Bureau, New York, 1987.

13. D. Wilson, H.D. Stenzenberger, P.M. Hergenrother, Polyimides, Blackie, Glasgow, 1990.

14. M.K. Ghosh, K.L. Mittal, Polyimides: Fundamentals and Applications, Marcel Dekker, New York, 1996.

15. L.S. White, T.A. Blinka, H.A. Kloczewski, I.-F Wang, Properties of a polyimide gas separation membrane in natural gas treams, J. Membr. Sci. 103 (1995) 73–82.

16. A. Bos, I.G.M. Punt, M. Wessling, H. Strathmann, Plasticization resistant glassy polyimide membranes for CO_2/CH_4 Separations, Sep. Purif. Technol. 14 (1998) 27–39.

17. A. Tena, L. Fernández, M. Sánchez, L. Palacio, A.E. Lozano, A. Hernández, P. Prádanos, Mixed matrix membranes of 6FDA-6FpDA with surface functionalized gamma-alumina particles. An analysis of the improvement of permselectivity for several gas pairs, Chem. Eng. Sci. 65 (6) (2010) 2227–2235.

18. K. Okamoto, N. Yasugi, T. Kawabata, K. Tanaka, H. Kita, Selective permeation of carbon dioxide through amine-modified polyimide membranes, Chem. Lett. 8 (1996) 613–614.

19. C. Staudt-Bickel, W.J. Koros, Improvement of CO_2/CH_4 separation characteristics of polyimides by chemical crosslinking, J. Membr. Sci. 155 (1999) 145–154.

20. L.M. Robeson, Correlation of separation factor versus permeability for polymeric membranes, J. Membr. Sci. 62 (1991) 165-185.

21. L.M. Robeson, The upper bound revisited, J. Membr. Sci. 320 (2008) 390–400

22. H.B. Park, C.H. Jung, Y.M. Lee, A.J. Hill, S.J. Pas, S.T. Mudie, E.V. Wagner, B.D. Freeman, D.J. Cookson, Polymers with cavities tuned for fast selective transport of small molecules and ions, Science 318 (2007) 254–258.

23. P.M. Budda, K.J. Msayib, C.E. Tattershall, B.S. Ghanema,K.J. Reynolds, N.B. McKeownb, D. Fritsch, Gas separation membranes from polymers of intrinsic microporosity, J.Membrane Sci. 251 (2005) 263–269

24. K. Ghosal, R.T. Chen, B.D. Freeman, W.H. Daly, I.I. Negulescu, Effects of basic substituents on gas sorption and permeation in polysulfone, Macromolecules 29 (1996) 4360–4369.

25. M. Kawakami , H. Iwanaga, Y. Hara, M. Iwamoto, S. J. Kagawa, Gas permeabilities of cellulose nitrate/poly(ethylene glycol) blend membranes, J. Appl. Polym. Sci. 27 (1982) 2387-2393.

26. J. Li, K. Nagai, T. Nakagawa, S. Wang, Preparation of Polyethyleneglycol (PEG) and Cellulose Acetate (CA) Blend Membranes and Their Gas Permeabilities, J. Appl. Polym. Sci. 58 (1995) 1455-1463.

27. H. Lin, B.D. Freeman, Gas solubility, diffusivity and permeability in poly(ethylene oxide), J. Membr. Sci. 239 (2004) 105-117.

28. H. Lin, E. van Wagner, J.S. Swinnea, B.D. Freeman, S.J. Pas, A.J. Hill, S. Kalakkunnath, D.S. Kalika, Transport and structural characteristics of crosslinked poly(ethylene oxide) rubbers, J. Membr. Sci. 276(1-2) (2006) 145-161.

29. Y. Hirayama, Y. Kase, N. Tanihara, Y. Sumiyama, Y. Kusuki, K. Haraya, Permeation properties to CO_2 and N_2 of poly(ethylene oxide)-containing and crosslinked polymer films, J. Membr. Sci. 160 (1999) 87-99.

30. J.J. Richards, M.K. Danquah, S. Kalakkunnath, D.S. Kalika, V.A. Kusuma, S.T. Matteucci, B.D. Freeman, Relation between structure and gas transport properties of polyethylene oxide networks based on crosslinked bisphenol A ethoxylate diacrylate, Chem. Eng. Sci. 64 (2009) 4707-4718

31. V.I. Bondar, B.D. Freeman, I. Pinnau, Gas sorption and characterization of poly(ether-b-amide) segmented block copolymers, J. Polym. Sci. Part B: Polym. Phys. 37 (1999) 2463-2475.

32. V.I. Bondar, B.D. Freeman, I. Pinnau, Gas transport properties of poly(ether-b-amide) segmented block copolymers, J. Polym. Sci. Part B: Polym. Phys. 38 (15) (2000) 2051-2062.

33. K. Okamoto, M. Fujii, S. Okamyo, H. Suzuki, K. Tanaka, H. Kita, Gas permeation properties of poly(ether imide) segmented copolymers, Macromolecules 28 (1995) 6950-6956.

34. Y. Hirayama, Y. Kase, N. Tanihara, Y. Sumiyama, Y. Kusuki, K. Haraya, Permeation properties to CO_2 and N_2 of poly(ethylene oxide)-containing and crosslinked polymer films, J. Membr. Sci. 160 (1999) 87-99.

35. M. Yoshino, K. Ito, H. Kita, K. Okamoto, Effects of hard-segment polymers on CO_2/N_2 gas separation properties of poly(ethylene oxide)-segmented copolymers, J. Polym. Sci. Part B: Polym. Phys. 38 (2000) 1707-1715.

36. H. Suzuki, K. Tanaka, H. Kita, K. Okamoto, H. Hoshino, T. Yoshinaga, Y. Kusuki, Preparation of composite hollow fiber membranes of poly(ethylene oxide)-containing polyimide and their CO_2/N_2 separation properties, J. Membr. Sci. 146 (1998) 31-37.

37. K. Okamoto, N. Umeo, S. Okamyo, K. Tanaka, H. Kita, Selective permeation of carbon dioxide over nitrogen through polyethyleneoxide-containing polyimide membranes, Chem. Lett. 5 (1993) 225-228.

38. C. Hangzheng, X. Youchang, C. Tai-Shung, Synthesis and characterization of poly (ethylene oxide) containing copolyimides for hydrogen purification, Polymer 51 (2010) 4077-4086

39. D.M. Muñoz, E.M. Maya, J. de Abajo, J.G. de la Campa, A.E. Lozano, Thermal treatment of poly(ethylene oxide)-segmented copolyimide based membranes: An effective way to improve the gas separation properties, J. Memb. Sci. 323 (2008) 53–59

40. A. Marcos-Fernandez, A. Tena, A.E. Lozano, J.G. de la Campa, J. de Abajo, L. Palacio, P. Prádanos, A. Hernández, Physical properties of films made of copy(ether-imide) with long poly(ethylene oxide) segments, Eur. Polym. J. 46 (2010) 2352-2374.

41. E.M. Maya, D.M. Muñoz, A.E. Lozano, J. de Abajo, J.G. de La Campa. Fluorenyl cardo copolyimides containing poly(ethylene oxide) segments: synthesis, characterization, and evaluation of properties. J. Polym. Sci. Part A: Polym. Chem. 46, (2008) 8170–8178

42. P.J. Haines, Thermal Methods of Analysis Principles, Applications and Problems, Chapman & Hall, New York, USA, 1995.

43. J. Marchese, M. Anson, N.A. Ochoa, P. Prádanos, L. Palacio, A. Hernández, Morphology and structure of ABS membranes filled with two different activated carbons, Chem. Eng. Sci. 61 (2006) 5448–5454.

44. H.A. Daynes, The process of diffusion through a rubber membrane, Proc. R. Soc. London 97 (1920) 286–307.

45. D. Paul, A.T. DiBenedetto, Gas and vapor solubility in crosslinked poly(ethylene glycol diacrylate), diffusion in amorphous polymers,. J. Polym. Sci. C 10 (1) (1965) 17–44.

46. J. Crank, The Mathematics of Diffusion, second ed Clarendon Press, Oxford, 1975

47. S.W. Rutherford, D.D. Do, Review of time-lag permeation technique as a method for characterization of porous media and membranes, Adsorpt. 3 (1997) 283–312.

48. J. Scheirs, S.W. Bigger, O. Delatycki, Characterizing the solid-state thermal oxidation of poly(ethylene oxide) powder, Polymer 32 (1991) 2014–2019.

49. M.A.B. Meador, V.A. Cubon, D.A. Scheiman, W.R. Bennett, Effect of branching on rod−coil block polyimides as membrane materials for lithium polymer batteries, Chem. Mater. 15 (15) (2003) 3018-3025

50. J.L. Hedrick, T. P. Russell, J. Labadie, M. Lucas, S. Swanson, High temperature nanofoams derived from rigid and semi-rigid polyimides. Polymer 36 (1995) 2685-2697

51. Y. Hu, M. Rogunova, V. Topolkaraev, A. Hiltner, E. Baer, Aging of poly(lactide)/poly(ethylene glycol) blends. Part 1. Poly(lactide) with low stereoregularity, Polymer 44 (2003) 5701–5710.

52. D.W.Van Krevelen, Properties of polymers, 3rd Ed. Amsterdam, Elsevier, p. 120 1990.

53. F.S. Baltá-Calleja, C.G.Vonk, X-ray scattering of synthetic polymers, Amsterdam, Elsevier, 1989.

54. L.S. Teo, C.Y. Chen, J.F. Kuo, The gas transport properties of amine-containing polyurethane and poly(urethane-urea) membranes, J. Membr. Sci. 141 (1998) 91-99.

55. P.M. Budd, K.J. Msayib, C.E. Tattershall, B.S. Ghanem, K.J. Reynolds, N.B. McKeown, D. Fritsch, Gas separation membranes from polymers of intrinsic microporosity, J. Membr. Sci. 251 (2005) 263.

56. T.C. Merkel, V. Bondar, K. Nagai, B.D. Freeman, Sorption and transport of hydrocarbon and perfluorocarbon gases in poly(1-trimethylsilyl-1-propyne), J. Polym. Sci. Part B: Polym. Phys. 38 (2000) 273-296.

57. L.G. Toy, K. Nagai, B.D. Freeman, I. Pinnau, Z. He, T. Masuda, M. Teraguchi, Y.P. Yampolskii, Pure-gas and vapor permeation and sorption properties of poly[1-phenyl-2-[p-(trimethylsilyl)phenyl]acetylene](PTMSDPA), Macromolecules 33 (2000) 2516-2524.

58. K. Nagai, A. Higuchi, T. Nakagawa, Gas permeability and stability of poly(1-trimethylsilyl-1-propyne-co-1-phenyl-1-propyne) membranes, J. Polym. Sci. Part B: Polym. Phys. 33 (1995) 289-298.

59. J.J. Richards, M.K. Danquah, S. Kalakkunnath, D.S. Kalika, V.A. Kusuma, S.T. Matteucci, B.D. Freeman, Relation between structure and gas transport properties of polyethylene oxide networks based on crosslinked bisphenol A ethoxylate diacrylate, Chem. Eng. Sci. 64(22) (2009) 4707-4718

60. R. Recio, , A.E. Lozano, P. Pradanos, A. Marcos, F. Tejerina, A. Hernandez, Effect of fractional free volume and Tg on gas separation through membranes made with different glassy polymers. J. Appl. Polym. Sci. 107 (2008) 1039–1046.

61. M. Sadeghi, M.A. Semsarzadeh, H. Moadel, Enhancement of the gas separation properties of polybenzimidazole (PBI) membrane by incorporation of silica nano particles, J. Membr. Sci. 331 (2009) 21–30.

62. H. Lin, B.D. Freeman, gas and vapor solubility in crosslinked Poly(ethylene glycol diacrylate), Macromolecules, 38 (2005) 8394-8407.

63. D.W. Breck, Zeolite Molecular Sieves: Structure, Chemistry and Use. Wiley, New York, NY. 1974.

FIGURE CAPTIONS

Figure 1. Chemical structure of the monomers.

Figure 2. Typical FTIR spectra showing the difference between imidized and not imidized cPI-ODA.

Figure 3. TGA curves in dynamic conditions for copolymers from different aromatic diamines treated at 160 ºC for 2 hours.

Figure 4. Glass transition temperatures as a function of the treatment temperature.

Figure 5. Melting temperatures as a function of the treatment temperature.

Figure 6. Q' and L as a function of the treatment temperature for the copolymer containing ODA. In graph (b), L differences for membranes treated at 120 and 160 ºC are compared.

Figure 7. Examples of Q' (PPD containing copolymer) (a) and L (BNZ) (b) as a function of the treatment temperature. Crosses correspond to samples treated in an oven at the temperatures depicted in the graph (samples were measured at ambient temperature).

Figure 8. Evolution of Q'_r and L as a function of temperature of treatment.

Figure 9. CO_2 permeability versus treatment temperature for the BNZ copolymer.

Figure 10. (a) Robeson's plot for the O_2/N_2 gas pair, (b) selectivity by solubility as a function of the selectivity by diffusivity. Stars correspond to pure PEO values.

Figure 11. (a) Robeson's plot for the CO_2/CH_4 gas pair, (b) selectivity by solubility as a function of the selectivity by diffusivity. Stars correspond to pure PEO values.

Figure 12. (a) Robeson's plot for the CO_2/N_2 gas pair, (b) selectivity by solubility as a function of the selectivity by diffusivity. Stars correspond to pure PEO values.

Figure 13. (a) Robeson's plot for the CH_4/N_2 gas pair, (b) selectivity by solubility as a function of the selectivity by diffusivity. Stars correspond to pure PEO values.

Figure 14. Solubility and diffusivity of methane as a function of the temperature of treatment.

TABLES

Table I. Synthesis details of aromatic-aliphatic copolyimides

Copolymer	Reactants *			Aromatic amine/aliphatic amine Molar ratio	% PEO by weight
	BPDA	Aromatic amine	PEO-2000**		
cPI-PPD	1.3026	0.4308	0.8614	8.98 : 1	34.6
cPI-BNZ	0.9445	0.4969	0.9968	5.25 : 1	42.9
cPI-ODA	0.9441	0.5336	1.0565	4.90 : 1	43.7

* Grams of reactants added in the synthesis for a 10 ml NMP solution. Molar ratio dianhydride : total diamines = 1 : 1. Weight ratio PEO-2000 : aromatic diamine = 2 : 1

** Mn = 1942 (by titration, given by the supplier)

Table II. Hard segment T_g as obtained by TMA for some temperatures of treatment.

Copolymer	Treatment T / ºC	Tg / ºC
cPI-PPD	160	208
cPI-ODA	120	140
	160	180
cPI-BNZ	120	150
	160	242

Table III. Mechanical properties at ambient temperature for the films treated at 160ºC for 2h.

Copolymer	cPI-PPD	cPI-BNZ	cPI-ODA
Maximum stress / MPa	61.5 ± 2.5	6.2 ± 1.9	22.1 ± 1.7
Strain / %	26 ± 10	1.1 ± 0.3	115 ± 53
Modulus / GPa	1.25 ± 0.09	0.65 ± 0.16	0.38 ± 0.04

Table IV. Permeabilities and selectivities for copolymers with different PEO length treated at 250ºC*

P_{O2}		P_{N2}		P_{CO2}		P_{CH4}		$\alpha\ O_2/N_2$		$\alpha\ CO_2/N_2$		$\alpha\ CO_2/CH_4$	
PI43	cPI-ODA	PI43	cPI-ODA	PI43	cPI-ODA	PI43	cPI-ODA	PI43	cPI-ODA	PI43	cPI-ODA	PI43	cPI-ODA
3.06	2.15	1.21	0.72	67	43.7	4.02	2.21	2.50	2.98	55	60.7	17	19.7

* PI43 results taken from reference 39

Table V. Kinetic diameter and boiling temperature of tested gases.

	Gas kinetic diameter (Å)	Critical temperature (K)
Carbon dioxide	3.30	304.2
Oxygen	3.46	154.6
Nitrogen	3.64	126.2
Methane	3.80	191.1

Figure

Figure 1

Dianhydride

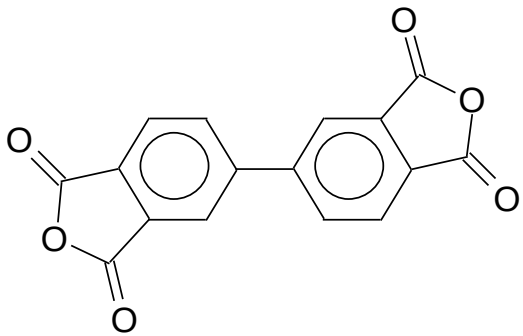

BPDA

Aliphatic diamine

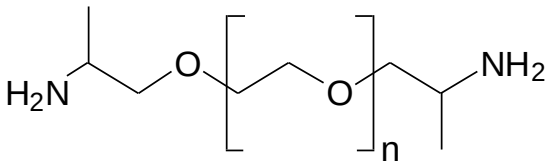

PEO-2000 (diamine terminated)

Aromatic diamines

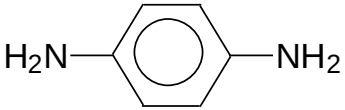

PPD

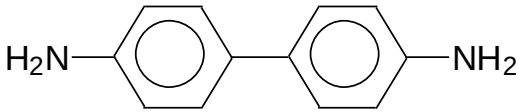

BNZ

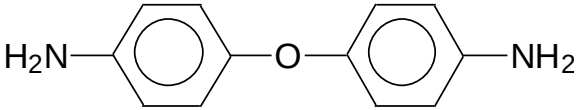

ODA

Figure 1. Chemical structure of the monomers

Figure 2

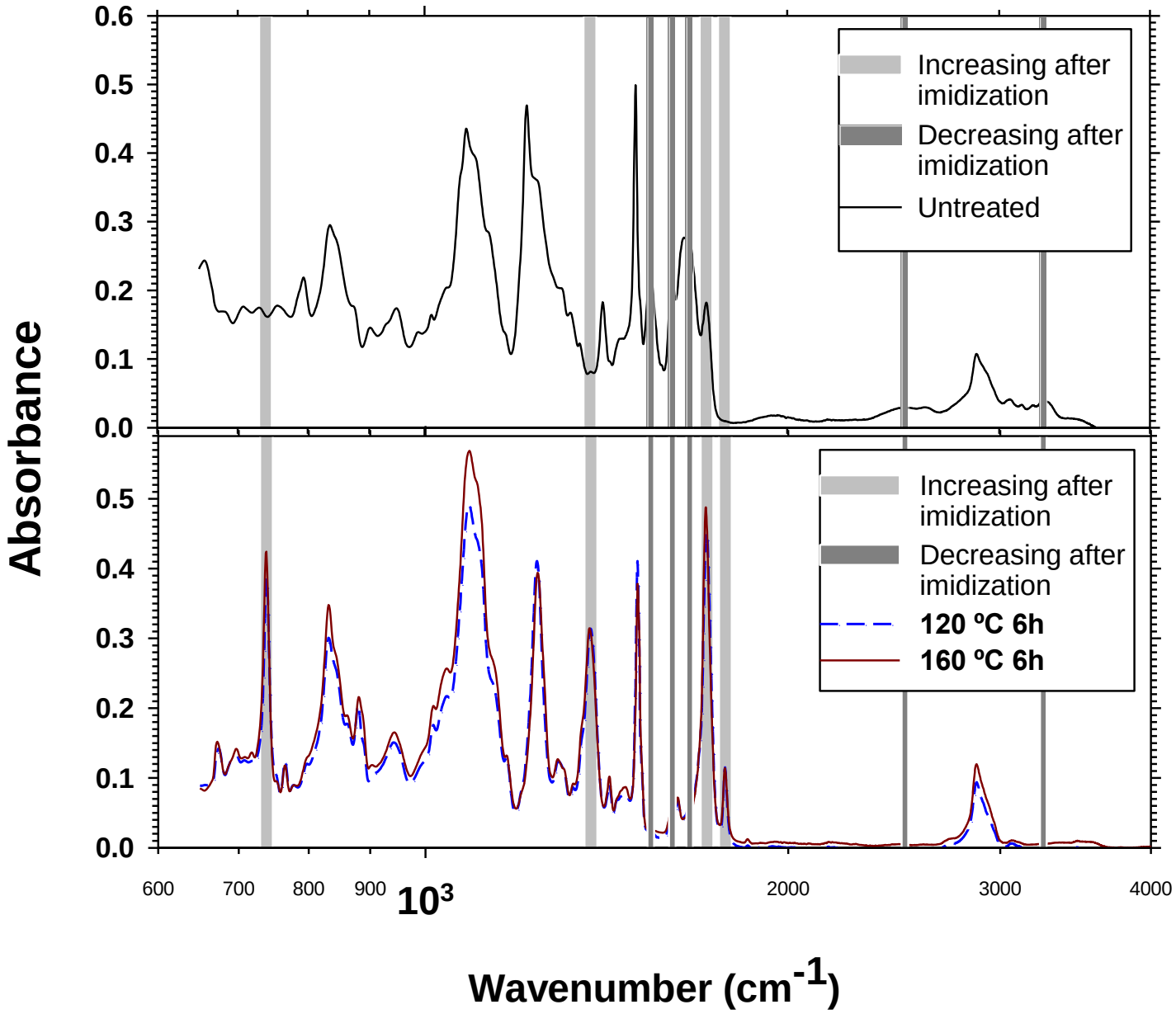

Figure 2. Typical FTIR spectra showing the difference between imidized and not imidized cPI-ODA. .

Figure 3

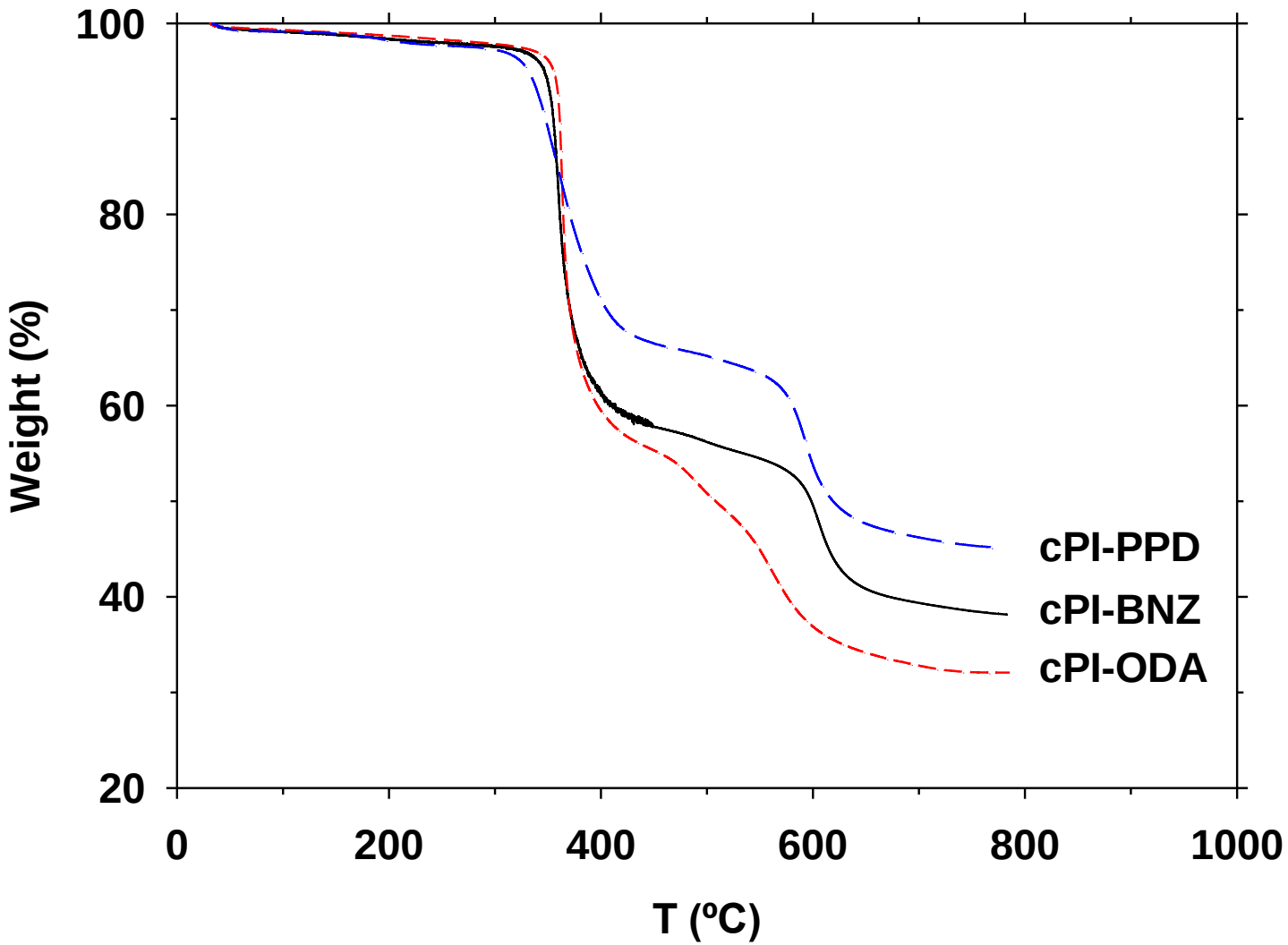

Figure 3. TGA curves in dynamic conditions for copolymers from different aromatic diamines treated at 160 ºC for 2 hours.

Figure 4

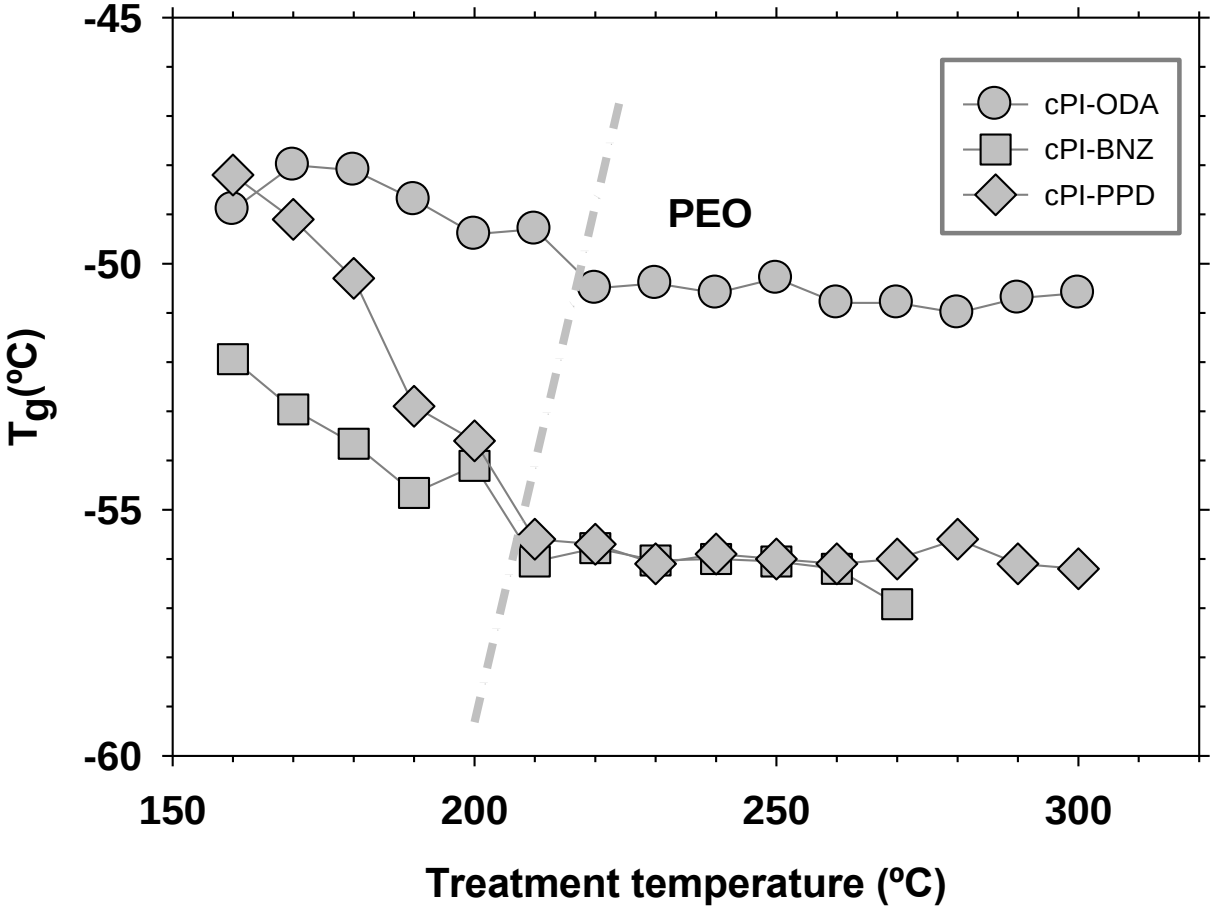

Figure 4. Glass transition temperatures as a function of the treatment temperature.

Figure 5

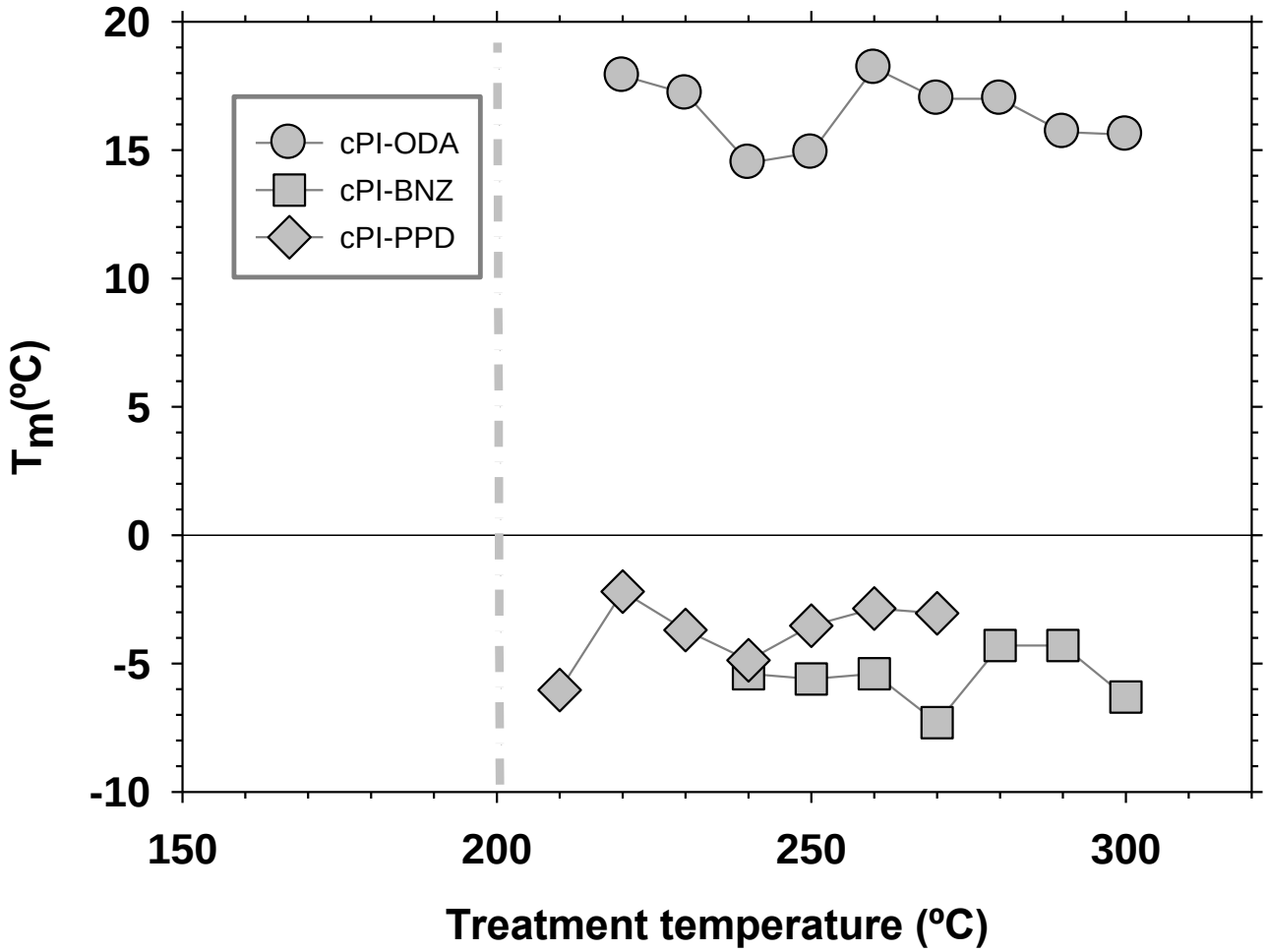

Figure 5. Melting temperatures as a function of the treatment temperature.

Figure 6

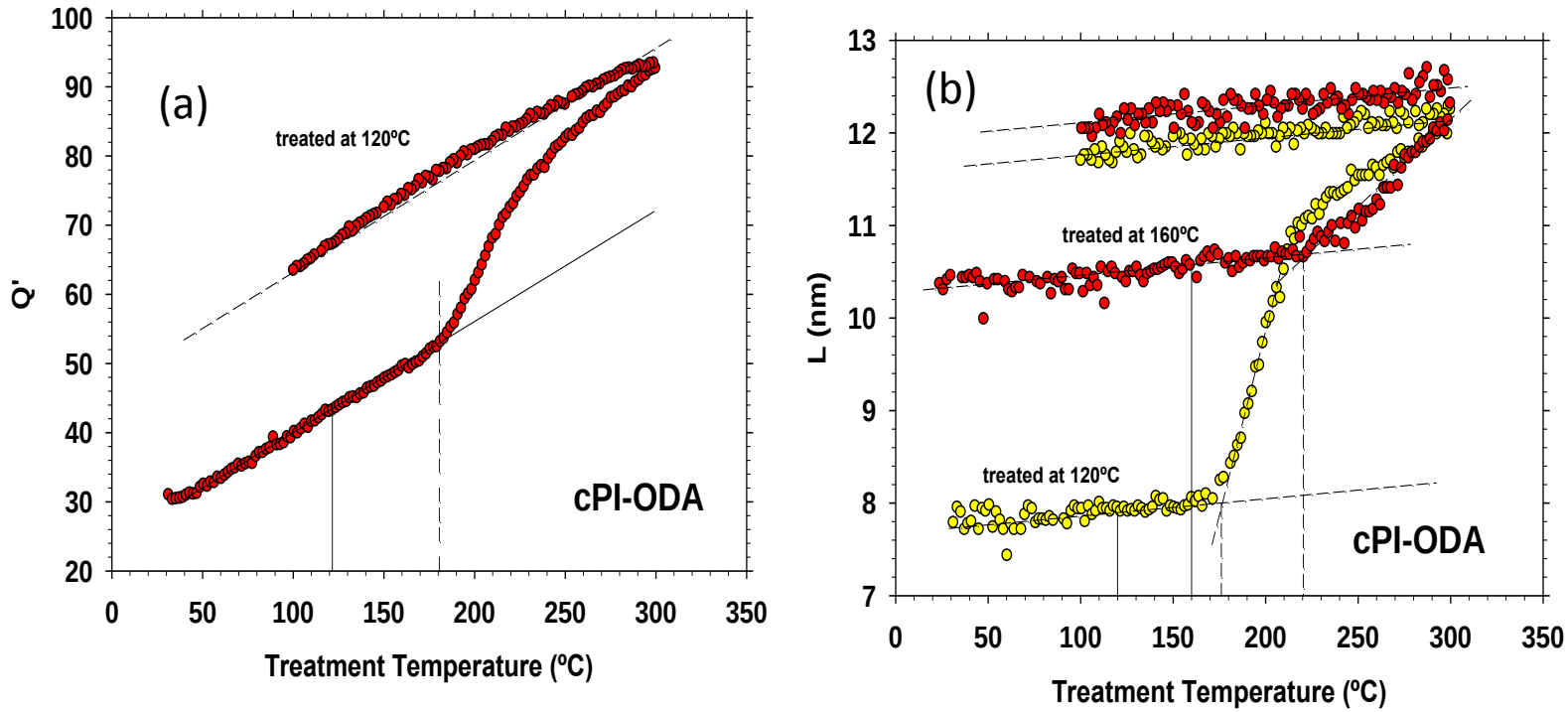

Figure 6. Q' and L as a function of the treatment temperature for the copolymer containing ODA. In graph (b), L differences for membranes treated at 120 and 160 ºC are compared.

Figure 7

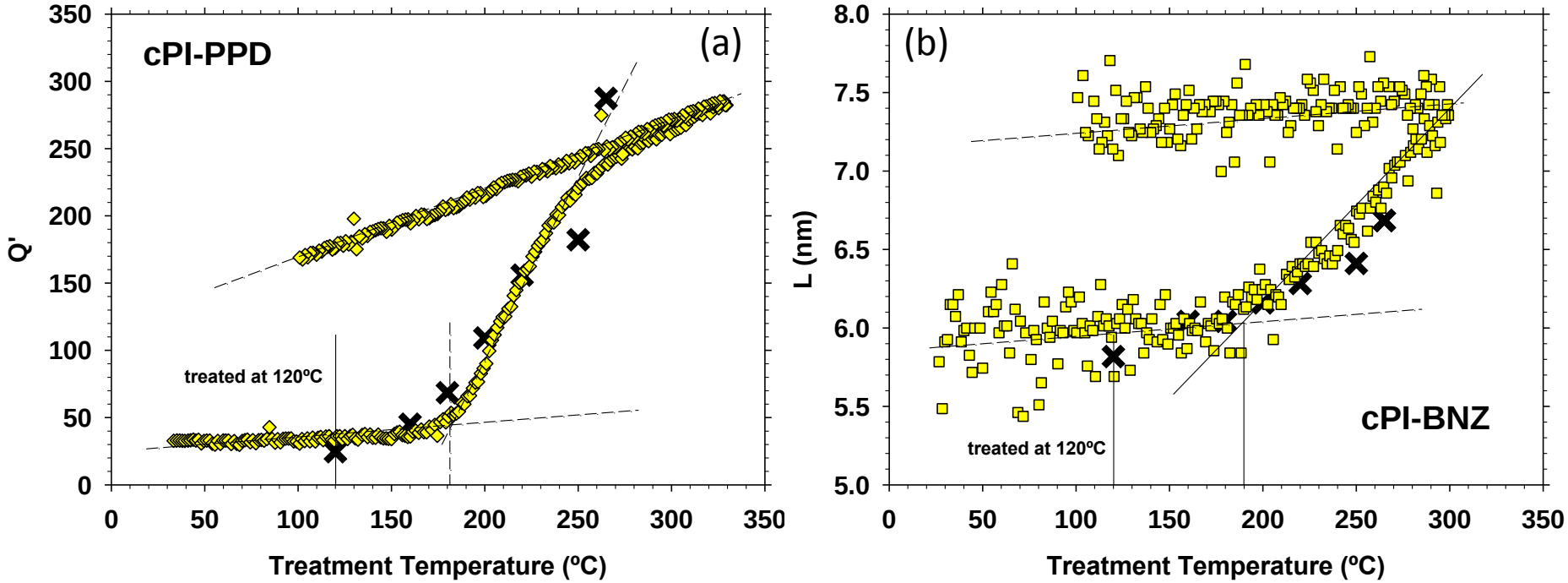

Figure 7. Examples of Q' (cPI-PPD) (a) and L (cPI-BNZ) (b) as a function of the treatment temperature. Crosses correspond to samples treated in an oven at the temperatures depicted in the graph (samples were measured at ambient temperature).

Figure 8

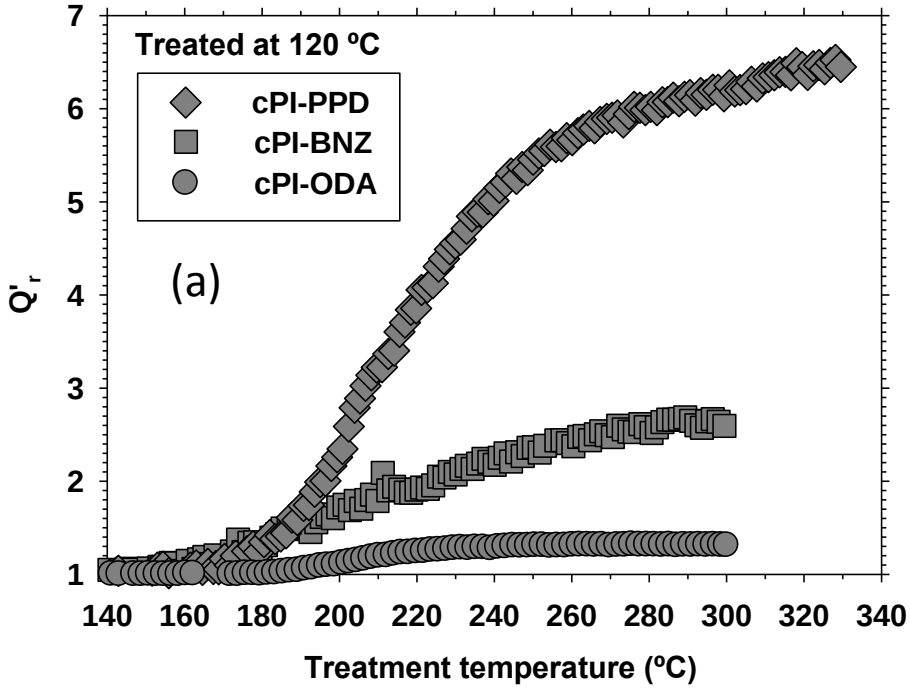

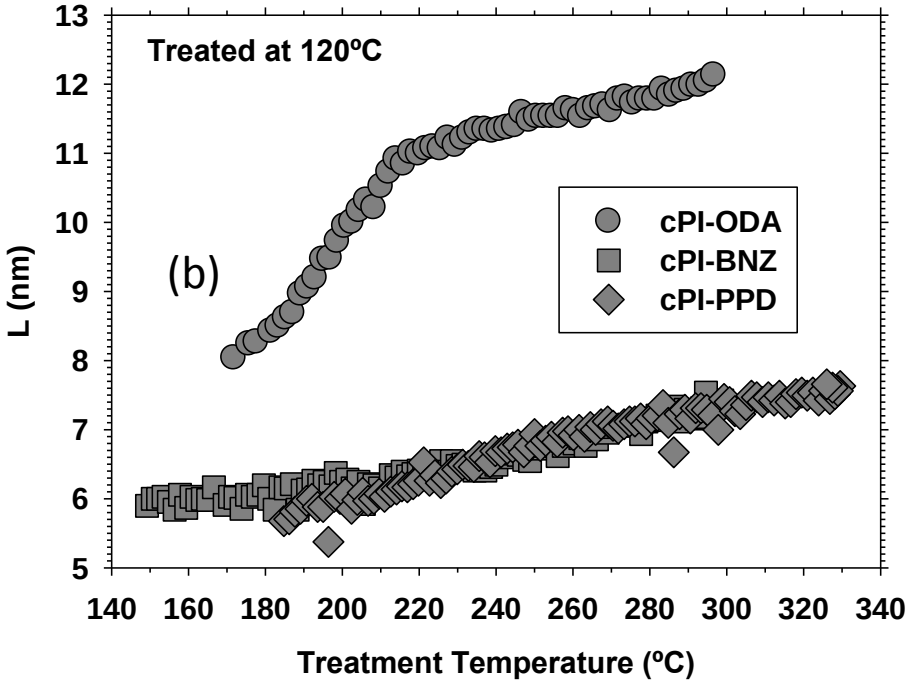

Figure 8. Evolution of Q'_r and L as a function of temperature of treatment.

Figure 9

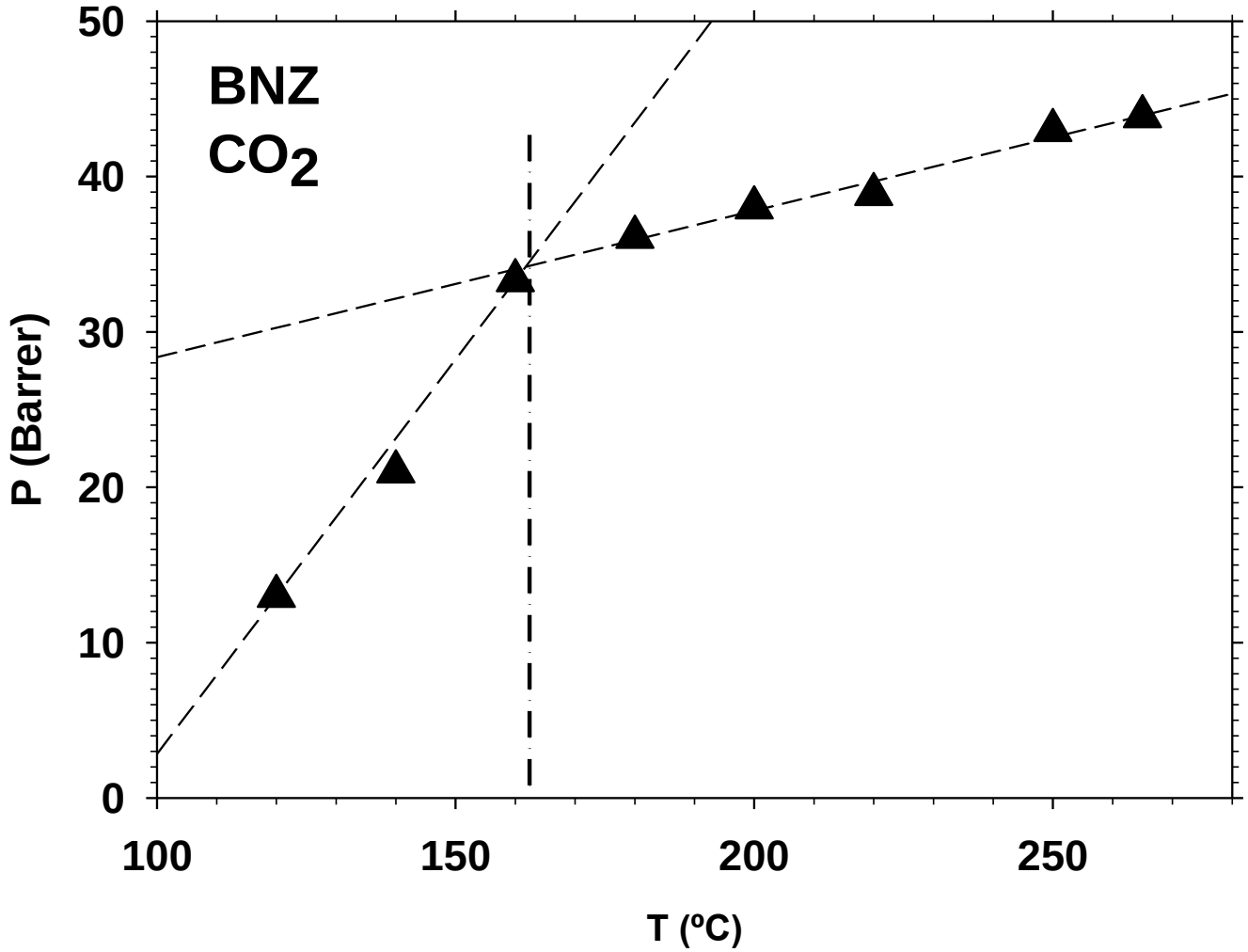

Figure 9. CO_2 permeability versus treatment temperature for the BNZ copolymer.

Figure 10

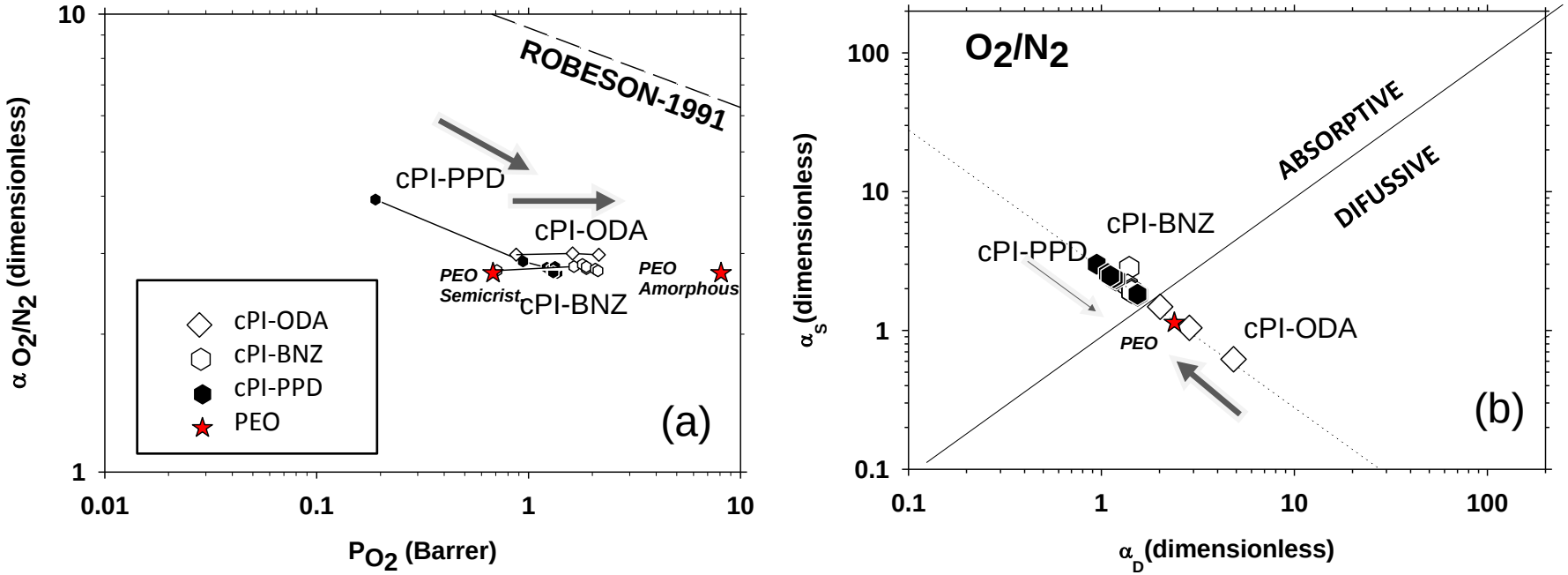

Figure 10. (a) Robeson's plot for the O_2/N_2 gas pair, (b) selectivity by solubility as a function of the selectivity by diffusivity. Stars correspond to the PEO values.

Figure 11

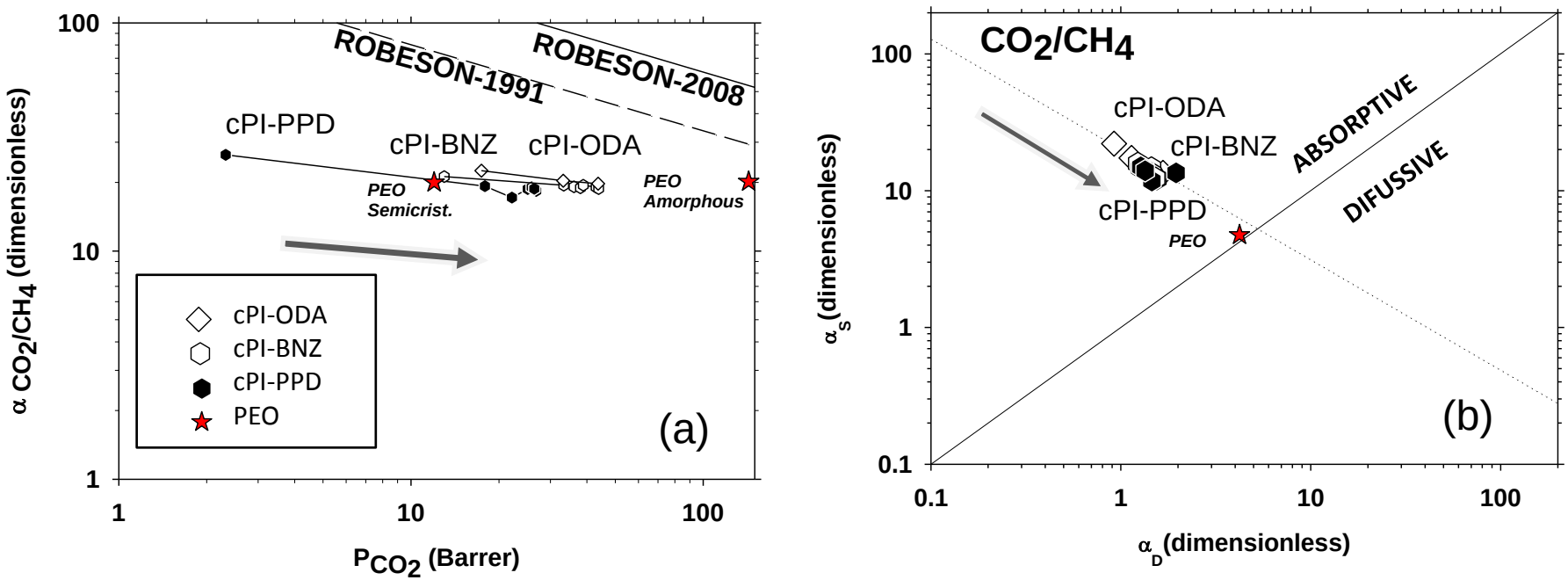

Figure 11. (a) Robeson's plot for the CO_2/CH_4 gas pair, (b) selectivity by solubility as a function of the selectivity by diffusivity. Stars correspond to pure PEO values.

Figure 12

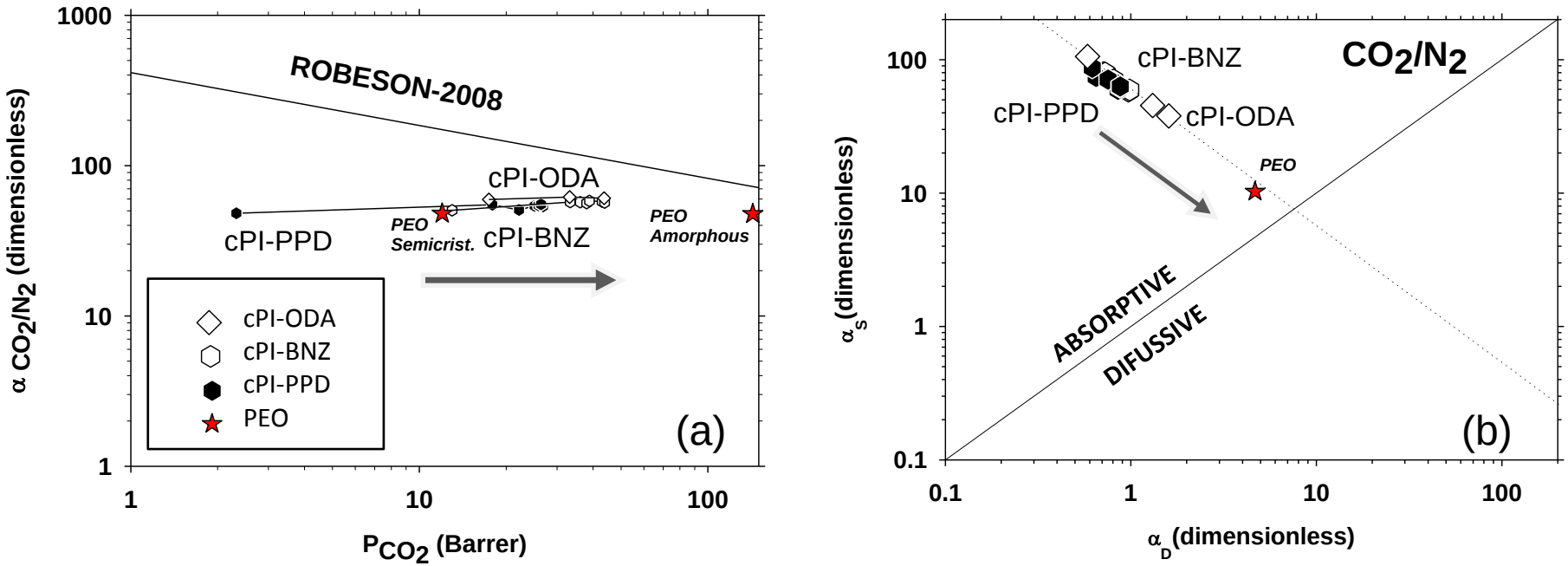

Figure 12. (a) Robeson's plot for the CO_2/N_2 gas pair, (b) selectivity by solubility as a function of the selectivity by diffusivity. Stars correspond to the PEO values.

Figure 13

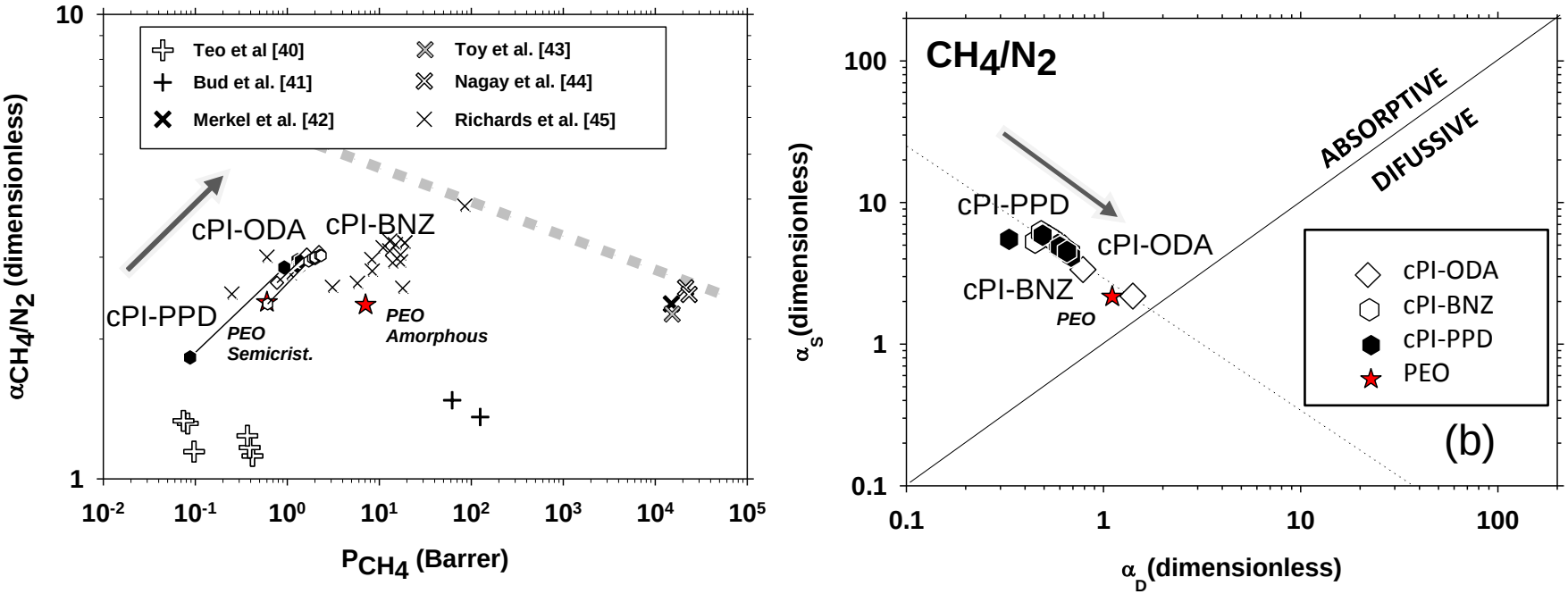

Figure 13. (a) Robeson's plot for the CH_4/N_2 gas pair, (b) selectivity by solubility as a function of the selectivity by diffusivity. Stars correspond to pure PEO values.

Figure 14

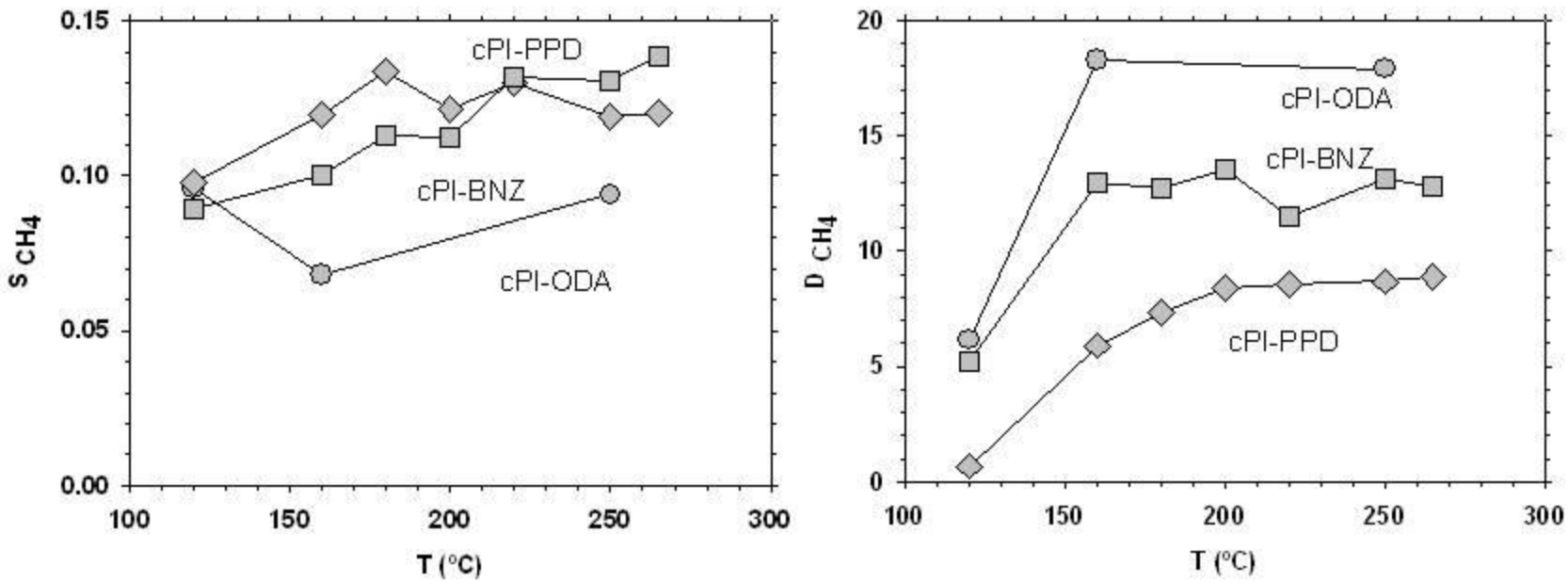

Figure 14 Solubility and diffusivity of methane as a function of the temperature of treatment.